alternative pathway from PGC-1 because MIDAS did not enhance mitochondrial transcription (Fig. 7C).

As mitochondria dynamically repeat fusion and fission, it is difficult to clarify their number (Griparic and van der Bliek, 2001; Westermann, 2002). In this study, we thus paid attention to the total mass of mitochondria. Three-dimensional imaging revealed a change in the total mass of mitochondria. The increase was 1.6-fold, which agrees with the increase in strength of the fluorescence of MitoTracker Red and MitoTracker Green in MIDAS-expressing transfectants. This increase is not so small because mitochondria occupy more than 20% of the total volume of the cytoplasm in HeLa cells. When the downregulation and upregulation of MIDAS were compared, the total mass was found to vary more than 2.3-fold from 15% to 35% of the total cytoplasm of HeLa cells. Thus, MIDAS dramatically regulates the total mitochondrial mass.

Mitochondria are often swollen pathogenically or by an increase of cytosolic Ca^{2+}. It may be that the mitochondria are simply swollen owing to the expression of MIDAS. However, this is unlikely for the following reasons. First, the ratio of the intensity in red to the intensity in green was the same in all the cells examined, indicating that MIDAS does not exert any influence on membrane potential (Fig. 6C). Although MIDAS-expressing cells have lower concentrations of mitochondrial protein per volume than controls (Fig. 7C), the levels seem high enough for membrane potential. Second, the downregulation of MIDAS conversely decreased the total mass of mitochondria. Third, mitochondria appear intact morphologically, being independent of the up- or downregulation of MIDAS (Fig. 5C). Finally, it is crucial that the amount of cardiolipin varied depending upon the amount of MIDAS and that the extent of the change was well correlated with the total mass of mitochondria that was revealed by three-dimensional imaging. Cardiolipin is a mitochondrion-specific lipid but accounts for only 20% of mitochondrial lipids. This suggests that not only the amount of cardiolipin but also the total amount of mitochondrial lipids is changed by MIDAS. Taken together, it is concluded that total mitochondrial mass is regulated by MIDAS through the biogenesis of mitochondrial lipids.

The molecular mechanism by which the MIDAS protein increases production of cardiolipin is unknown. A detailed analysis of the *MIDAS* gene and the function of MIDAS should provide insight into the molecular mechanism by which mitochondrial dysfunction is sensed to increase mitochondria. The fact that MIDAS is colocalized with both mitochondria and the Golgi apparatus may be a key to answering the question of how lipids contribute to mitochondrial accumulation.

We thank K. Mihara of Kyushu University for the gift of anti-Tom20 and anti-Tom40 antibodies, I. Ohsawa and T. Kanamori for helpful advice and K. Yamagata for technical assistance.

References

Amuthan, G., Biswas, G., Zhang, S. Y., Klein-Szanto, A., Vijayasarathy, C. and Avadhani, N. G. (2001). Mitochondria-to-nucleus stress signaling induces phenotypic changes, tumor progression and cell invasion. *EMBO J.* **20**, 1910-1920.

Asoh, S., Mori, T., Hayashi, J. and Ohta, S. (1996). Expression of the apoptosis-mediator Fas is enhanced by dysfunctional mitochondria. *J. Biochem. (Tokyo)* **120**, 600-607.

Attardi, G. and Schatz, G. (1988). Biogenesis of mitochondria. *Annu. Rev. Cell Biol.* **4**, 289-333.

Bell, A. W., Ward, M. A., Blackstock, W. P., Freeman, H. N., Choudhary, J. S., Lewis, A. P., Chotai, D., Fazel, A., Gushue, J. N., Paiement, J. et al. (2001). Proteomics characterization of abundant Golgi membrane proteins. *J. Biol. Chem.* **276**, 5152-5165.

Bereiter-Hahn, J. and Voth, M. (1994). Dynamics of mitochondria in living cells: shape changes, dislocations, fusion and fission of mitochondria. *Microsc. Res. Tech.* **27**, 198-219.

Bidlingmaier, S. and Snyder, M. (2002). Large-scale identification of genes important for apical growth in *Saccharomyces cerevisiae* by directed allele replacement technology (DART) screening. *Funct. Integr. Genomics* **1**, 345-356.

Biswas, G., Adebanjo, O. A., Freedman, B. D., Anandatheerthavarada, H. K., Vijayasarathy, C., Zaidi, M., Kotlikoff, M. and Avadhani, N. G. (1999). Retrograde Ca^{2+} signaling in C2C12 skeletal myocytes in response to mitochondrial genetic and metabolic stress: a novel mode of inter-organelle crosstalk. *EMBO J.* **18**, 522-533.

Bonangelino, C. J., Chavez, E. M. and Bonifacino, J. S. (2002). Genomic screen for vacuolar protein sorting genes in *Saccharomyces cerevisiae*. *Mol. Biol. Cell* **13**, 2486-2501.

Brunk, C. F. (1981). Mitochondrial proliferation during myogenesis. *Exp. Cell Res.* **136**, 305-309.

Collins, T. J., Berridge, M. J., Lipp, P. and Bootman, M. D. (2002). Mitochondria are morphologically and functionally heterogeneous within cells. *EMBO J.* **21**, 1616-1627.

Cortopassi, G. A. and Wong, A. (1999). Mitochondria in organismal aging and degeneration. *Biochim. Biophys. Acta* **1410**, 183-193.

Demple, B., Herman, T. and Chen, D. S. (1991). Cloning and expression of APE, the cDNA encoding the major human apurinic endonuclease: definition of a family of DNA repair enzymes. *Proc. Natl. Acad. Sci. USA* **88**, 11450-11454.

Dubowitz, V. (1985). Histological and histochemical stains and reactions. In *Muscle Biopsy: a practical approach*, 2nd edn, (ed. V. Dubowitz), pp. 19-40. London: Balliere Tindall.

Engel, W. K. and Cunningham, G. G. (1963). Rapid examination of muscle tissue. An improved trichrome method for fresh-frozen biopsy sections. *Neurology* **13**, 919-926.

Erlich, R., Gleeson, P. A., Campbell, P., Dietzsch, E. and Toh, B. H. (1996). Molecular characterization of *trans*-Golgi p230. A human peripheral membrane protein encoded by a gene on chromosome 6p12-22 contains extensive coiled-coil alpha-helical domains and a granin motif. *J. Biol. Chem.* **271**, 8328-8337.

Folch, J., Lees, M. and Sloane Stanley, G. H. (1957). A simple method for the isolation and purification of total lipides from animal tissues. *J. Biol. Chem.* **226**, 497-509.

Garesse, R. and Vallejo, C. G. (2001). Animal mitochondrial biogenesis and function: a regulatory cross-talk between two genomes. *Gene* **263**, 1-16.

Goglia, F., Moreno, M. and Lanni, A. (1999). Action of thyroid hormones at the cellular level: the mitochondrial target. *FEBS Lett.* **452**, 115-120.

Goto, Y., Nonaka, I. and Horai, S. (1990). A mutation in the $tRNA^{Leu(UUR)}$ gene associated with the MELAS subgroup of mitochondrial encephalomyopathies. *Nature* **348**, 651-653.

Green, D. R. and Kroemer, G. (2004). The pathophysiology of mitochondrial cell death. *Science* **305**, 626-629.

Griparic, L. and van der Bliek, A. M. (2001). The many shapes of mitochondrial membranes. *Traffic* **2**, 235-244.

Hansson, A., Hance, N., Dufour, E., Rantanen, A., Hultenby, K., Clayton, D. A., Wibom, R. and Larsson, N. G. (2004). A switch in metabolism precedes increased mitochondrial biogenesis in respiratory chain-deficient mouse hearts. *Proc. Natl. Acad. Sci. USA* **101**, 3136-3141.

Hasegawa, H., Matsuoka, T., Goto, Y. and Nonaka, I. (1991). Strongly succinate dehydrogenase-reactive blood vessels in muscles from patients with mitochondrial myopathy, encephalopathy, lactic acidosis and stroke-like episodes. *Ann. Neurol.* **29**, 601-605.

Hayashi, J., Ohta, S., Kikuchi, A., Takemitsu, M., Goto, Y. and Nonaka, I. (1991). Introduction of disease-related mitochondrial DNA deletions into HeLa cells lacking mitochondrial DNA results in mitochondrial dysfunction. *Proc. Natl. Acad. Sci. USA* **88**, 10614-10618.

Hayashi, J., Ohta, S., Kagawa, Y., Kondo, H., Kaneda, H., Yonekawa, H., Takai, D. and Miyabayashi, S. (1994). Nuclear but not mitochondrial genome involvement in human age-related mitochondrial dysfunction. Functional integrity of mitochondrial DNA from aged subjects. *J. Biol. Chem.* **269**, 6878-6883.

Holt, I. J., Harding, A. E. and Morgan-Hughes, J. A. (1988). Deletions of muscle mitochondrial DNA in patients with mitochondrial myopathies. *Nature* **331**, 717-719.

Jishage, M., Fujino, T., Yamazaki, Y., Kuroda, H. and Nakamura, T. (2003). Identification of target genes for EWS/ATF-1 chimeric transcription factor. *Oncogene* **22**, 41-49.

Kanamori, T., Nishimaki, K., Asoh, S., Ishibashi, Y., Takata, I., Kuwabara, T., Taira, K., Yamaguchi, H., Sugihara, S., Yamazaki, T. et al. (2003). Truncated product of the bifunctional *DLST* gene involved in biogenesis of the respiratory chain. *EMBO J.* **22**, 2913-2923.

Kang, D. and Hamasaki, N. (2002). Maintenance of mitochondrial DNA integrity: repair and degradation. *Curr. Genet.* **41**, 311-322.

Kawahara, H., Houdou, S. and Inoue, T. (1991). Scanning electron microscopic observations on muscle cells of experimental mitochondrial myopathy produced by **2**, 4-dinitrophenol. *J. Submicrosc. Cytol. Pathol.* **23**, 397-403.

Klaus, S., Casteilla, L., Bouillaud, F. and Ricquier, D. (1991). The uncoupling protein UCP: a membraneous mitochondrial ion carrier exclusively expressed in brown adipose tissue. *Int. J. Biochem.* **23**, 791-801.

Kobayashi, Y., Momoi, M. Y., Tominaga, K., Momoi, T., Nihei, K., Yanagisawa, M., Kagawa, Y. and Ohta, S. (1990). A point mutation in the mitochondrial $tRNA^{Leu(UUR)}$ gene in MELAS (mitochondrial myopathy, encephalopathy, lactic acidosis and stroke-like episodes). *Biochem. Biophys. Res. Commun.* **173**, 816-822.

Kobayashi, Y., Momoi, M. Y., Tominaga, K., Shimoizumi, H., Nihei, K., Yanagisawa, M., Kagawa, Y. and Ohta, S. (1991). Respiration-deficient cells are caused by a single point mutation in the mitochondrial $tRNA^{Leu(UUR)}$ gene in mitochondrial myopathy, encephalopathy, lactic acidosis and strokelike episodes (MELAS). *Am. J. Hum. Genet.* **49**, 590-599.

Kowaltowski, A. J. and Vercesi, A. E. (1999). Mitochondrial damage induced by conditions of oxidative stress. *Free Radic. Biol. Med.* **26**, 463-471.

Kroemer, G. and Reed, J. C. (2000). Mitochondrial control of cell death. *Nat. Med.* **6**, 513-519.

Liang, P. and Pardee, A. B. (1992). Differential display of eukaryotic messenger RNA by means of the polymerase chain reaction. *Science* **257**, 967-971.

Lightowlers, R. N., Chinnery, P. F., Turnbull, D. M. and Howell, N. (1997). Mammalian mitochondrial genetics: heredity, heteroplasmy and disease. *Trends Genet.* **13**, 450-455.

Melov, S. (2000). Mitochondrial oxidative stress. Physiologic consequences and potential for a role in aging. *Ann. New York Acad. Sci.* **908**, 219-225.

Moraes, C. T., Ricci, E., Bonilla, E., DiMauro, S. and Schon, E. A. (1992). The mitochondrial $tRNA^{Leu(UUR)}$ mutation in mitochondrial encephalomyopathy, lactic acidosis and strokelike episodes (MELAS): genetic, biochemical and morphological correlations in skeletal muscle. *Am. J. Hum. Genet.* **50**, 934-949.

Moyes, C. D., Mathieu-Costello, O. A., Tsuchiya, N., Filburn, C. and Hansford, R. G. (1997). Mitochondrial biogenesis during cellular differentiation. *Am. J. Physiol.* **272**, C1345-C1351.

Muller-Hocker, J., Pongratz, D. and Hubner, G. (1986). Activation of mitochondrial ATPase as evidence of loosely coupled oxidative phosphorylation in various skeletal muscle disorders. A histochemical fine-structural study. *J. Neurol. Sci.* **74**, 199-213.

Munro, S. and Pelham, H. R. (1987). A C-terminal signal prevents secretion of luminal ER proteins. *Cell* **48**, 899-907.

Nisoli, E., Clementi, E., Paolucci, C., Cozzi, V., Tonello, C., Sciorati, C., Bracale, R., Valerio, A., Francolini, M., Moncada, S. et al. (2003). Mitochondrial biogenesis in mammals: the role of endogenous nitric oxide. *Science* **299**, 896-899.

Nisoli, E., Falcone, S., Tonello, C., Cozzi, V., Palomba, L., Fiorani, M., Pisconti, A., Brunelli, S., Cardile, A., Francolini, M. et al. (2004). Mitochondrial biogenesis by NO yields functionally active mitochondria in mammals. *Proc. Natl. Acad. Sci. USA* **101**, 16507-16512.

Ohta, S. (2003). A multi-functional organelle mitochondrion is involved in cell death, proliferation and disease. *Curr. Med. Chem.* **10**, 2485-2494.

Pfanner, N. and Geissler, A. (2001). Versatility of the mitochondrial protein import machinery. *Nat. Rev. Mol. Cell. Biol.* **2**, 339-349.

Scarpulla, R. C. (2002). Nuclear activators and coactivators in mammalian mitochondrial biogenesis. *Biochim. Biophys. Acta* **1576**, 1-14.

Schon, E. A. (2000). Mitochondrial genetics and disease. *Trends Biochem. Sci.* **25**, 555-560.

Shoubridge, E. A., Karpati, G. and Hastings, K. E. (1990). Deletion mutants are functionally dominant over wild-type mitochondrial genomes in skeletal muscle fiber segments in mitochondrial disease. *Cell* **62**, 43-49.

Tong, A. H., Lesage, G., Bader, G. D., Ding, H., Xu, H., Xin, X., Young, J., Berriz, G. F., Brost, R. L., Chang, M. et al. (2004). Global mapping of the yeast genetic interaction network. *Science* **303**, 808-813.

Trounce, I. A., Kim, Y. L., Jun, A. S. and Wallace, D. E. (1996). Assessment of mitochondrial oxidative phosphorylation in patient muscle biopsies, lymphoblasts and transmitochondrial cell lines. *Methods Enzymol.* **264**, 484-509.

Vorobjev, I. A. and Zorov, D. B. (1983). Diazepam inhibits cell respiration and induces fragmentation of mitochondrial reticulum. *FEBS Lett.* **163**, 311-314.

Wallace, D. C. (1999). Mitochondrial diseases in man and mouse. *Science* **283**, 1482-1488.

Weber, K., Ridderskamp, D., Alfert, M., Hoyer, S. and Wiesner, R. J. (2002). Cultivation in glucose-deprived medium stimulates mitochondrial biogenesis and oxidative metabolism in HepG2 hepatoma cells. *Biol. Chem.* **383**, 283-290.

Wei, Y. F., Robins, P., Carter, K., Caldecott, K., Pappin, D. J., Yu, G. L., Wang, R. P., Shell, B. K., Nash, R. A., Schar, P. et al. (1995). Molecular cloning and expression of human cDNAs encoding a novel DNA ligase IV and DNA ligase III, an enzyme active in DNA repair and recombination. *Mol. Cell. Biol.* **15**, 3206-3216.

Westermann, B. (2002). Merging mitochondria matters: Cellular role and molecular machinery of mitochondrial fusion. *EMBO Rep.* **3**, 527-531.

Winzeler, E. A., Shoemaker, D. D., Astromoff, A., Liang, H., Anderson, K., Andre, B., Bangham, R., Benito, R., Boeke, J. D., Bussey, H. et al. (1999). Functional characterization of the *S. cerevisiae* genome by gene deletion and parallel analysis. *Science* **285**, 901-906.

Wu, C. C., Taylor, R. S., Lane, D. R., Ladinsky, M. S., Weisz, J. A. and Howell, K. E. (2000). GMx33: a novel family of *trans*-Golgi proteins identified by proteomics. *Traffic* **1**, 963-975.

Yaffe, M. P. (1999). The machinery of mitochondrial inheritance and behavior. *Science* **283**, 1493-1497.

Zeller, R. (1998). Preparation of cells and tissues for fluorescence microscopy. In *Cells: A Laboratory Manual. Volume 3 Subcellular localization of genes and their products.* (ed. D. L. Spector, R. D. Goldman and L. A. Leinwand), pp. 98.01-98.20. New York: Cold Spring Harbor Laboratory Press.

Journal of Cell Science

Cell Death and Differentiation (2005), 1–11

www.nature.com/cdd

Zonal necrosis prevented by transduction of the artificial anti-death FNK protein

S Asoh[1], T Mori[2], S Nagai[1], K Yamagata[1], K Nishimaki[1], Y Miyato[1], Y Shidara[1,3] and S Ohta*[,1]

[1] Department of Biochemistry and Cell Biology, Institute of Development and Aging Sciences, Graduate School of Medicine, Nippon Medical School, Kawasaki-city, Kanagawa, Japan
[2] Saitama Medical Center/School, Kawagoe, Saitama, Japan
[3] Department of Pathology, Tokyo Women's Medical University, School of Medicine, Shinjuku-ku, Tokyo, Japan
* Corresponding author: S Ohta, Department of Biochemistry and Cell Biology, Institute of Development and Aging Sciences, Graduate School of Medicine, Nippon Medical School, Kawasaki-city, Kanagawa 211-8533, Japan. Tel: +81 44 733 9267; Fax: +81 44 733 9268; E-mail: ohta@nms.ac.jp

Received 28.6.04; revised 15.11.04; accepted 26.11.04
Edited by H Ichijo

Abstract

Protection of cells from necrosis would be important for many medical applications. Here, we show protein transduction domain (PTD)-FNK therapeutics based on protein transduction to prevent necrosis and acute hepatic injury with zonal death induced by carbon tetrachloride (CCl_4). PTD-FNK is a fusion protein comprising the HIV/Tat PTD and FNK, a gain-of-function mutant of anti-apoptotic Bcl-x_L. PTD-FNK protected hepatoma HepG2 from necrotic death induced by CCl_4, and additionally, increased the apoptotic population among cells treated with CCl_4. A concomitant treatment with a pan-caspase inhibitor Z-VAD-FMK (N-benzyloxycarbonyl-Val-Ala-Asp-fluoromethylketone), which alone could not prevent the necrosis, protected these cells from the apoptosis. When pre-injected intraperitoneally, PTD-FNK markedly reduced zonal liver necrosis caused by CCl_4. Moreover, injection of PTD-FNK accompanied by Z-VAD-FMK suppressed necrotic injury even after CCl_4 administration. These results suggest that PTD-FNK has great potential for clinical applications to prevent cell death, whether from apoptosis or necrosis, and organ failure.

Cell Death and Differentiation advance online publication, 4 February 2005; doi:10.1038/sj.cdd.4401569

Keywords: necrosis; apoptosis; protein transduction domain; carbon tetrachloride; HepG2; liver; Bcl-x_L; protein therapeutics

Abbreviations: Ac-DEVD-AMC, *N*-acetyl-Asp-Glu-Val-Asp-7-amino-4-methylcoumarin; Ac-DEVD-CHO, *N*-acetyl-Asp-Glu-Val-Asp-CHO (aldehyde); ALT, alanine amino transferase; AST, aspartate amino transferase; CCl_4, carbon tetrachloride; DMEM, Dulbecco's modified Eagle's medium; ER, endoplasmic reticulum; *i.p.*, intraperitoneally; *s.c.*, subcutaneously; DEX, dexamethasone; TNFα, tumor necrosis factor α; CHX, cycloheximide; PARP-1, poly(ADP-ribose) polymerase; PI, propidium iodide; PTD, protein transduction domain; STS, staurosporine; Z-VAD-FMK, *N*-benzyloxycarbonyl-Val-Ala-Asp-fluoromethylketone; TUNEL, terminal deoxynucleotidyl transferase-mediated dUTP nick-end labeling

Introduction

Necrosis is morphologically distinct from apoptosis and defined as cell death accompanied by a rapid efflux of cell constituents to the extracellular space due to a loss of cytoplasmic membrane integrity.[1] Necrosis usually takes place under extremely harmful environmental conditions such as exposure to toxic chemicals, physical insults, and microbial pathogens and causes inflammation, which in turn gives rise to serious damage to surrounding cells.[2] Inflammatory responses can be controlled with anti-inflammatory agents, but necrosis itself cannot.[3–5] Therefore, it is very important to reduce or prevent necrosis as a primary cause.

Anti-apoptotic proteins would provide novel means for therapeutic intervention to prevent massive cell death accompanying cell toxic injuries. In fact, a great number of studies have shown that anti-apoptotic members of the Bcl-2 family, Bcl-2 and Bcl-x_L, inhibit apoptosis of cultured cells induced by various death stimuli.[6–11] On the other hand, a few *in vitro* studies[12,13] showed that the proteins prevent necrotic cell death caused by a limited kind of death stimulus such as hyposia, where necrosis coexists with apoptosis. In these cases, necrosis appeared to be initiated by apoptosis-inducing reagents, and then ATP depletion resulted in a necrotic morphology. Thus, the anti-apoptotic proteins seem to exhibit anti-cell death activity against some forms of necrosis, which involve apoptotic machinery to some extent.

FNK (originally designated Bcl-xFNK in Asoh *et al.*[14]) was constructed from Bcl-x_L by the site-directed mutagenesis of three amino acids (Y22*F*/ Q26*N*/ R165*K*) to strengthen cytoprotective activity. FNK is the sole mutant with a gain-of-function phenotype among the mammalian anti-apoptotic factors, as FNK exhibited the stronger anti-apoptotic activity than Bcl-x_L to protect cultured cells from death induced by various death stimuli including oxidative stress, a calcium ionophore (A23187) and withdrawal of growth factors.[14] It has been shown that proteins are directly and readily introduced into cells regardless of their molecular size when fused with the PTD (protein transduction domain) of HIV/Tat protein.[15] PTD-fused proteins can be delivered to several tissues, including the brain, when injected into mice systemically.[16] In addition, PTD-FNK, a fusion protein of the PTD and FNK, penetrates the dense matrix of cartilage to reach chondrocytes.[17] In a previous study, PTD-FNK was demonstrated to reduce ischemic injury to hippocampal CA1 neurons after a transient forebrain ischemia,[18] which involves slow progressive neuronal degeneration, and an apoptotic pathway is suggested to contribute to the ischemic degeneration, to some extent.[19]

The enhanced cytoprotective activity of FNK against oxidative stress and a calcium ionophore give rise to the possibility that FNK effectively protects cells from necrosis as well as apoptosis, because oxidative stress[20–22] and a disruption of calcium homeostasis[23–25] are known to induce necrosis. Carbon tetrachloride (CCl_4) has been used to induce necrosis in control experiments for studies on apoptosis[26–29] and is one of most typical model agents for studying the pathogenesis of liver injury. The hepatotoxicity of CCl_4 *in vivo* has been well studied, indicating the importance of the reductive dehalogenation of CCl_4 catalyzed by cytochrome P450 in the endoplasmic reticulum (ER) as the initial event of the toxic cascades,[30–34] and it is widely accepted that CCl_4 causes hepatic centrilobular necrosis.

Here, we show that the treatment of mice with PTD-FNK mitigated liver injury, including zonal necrosis, induced by CCl_4.

Results

Necrosis in HepG2 induced by CCl_4

We used a cell line HepG2 derived from hepatocyte cells as in *in vitro* experiments. HepG2 started to die in Dulbecco's modified Eagle's medium (DMEM) containing 80% saturation of CCl_4 in the absence of serum at 4 h and the survival rate at 8 h was 5.5% (Figure 1a). Thus, the CCl_4-induced death is not due to an immediate damage by CCl_4 as reported.[35] Nuclear staining with propidium iodide (PI)/Hoechst 33342 showed that PI-positive cells increased in number with time and that a majority of dead cells had a round nucleus uniformly stained with PI (Figure 1e). Their nuclear morphology is different from that of the cells killed by staurosporine (STS), which clearly caused nuclear fragmentation, one of the typical features of apoptosis (Figure 2c, top left panel). To characterize biochemically the death form of HepG2 cells treated with CCl_4, caspase-3/caspase-3-like activity, DNA fragmentation (laddering) and cleavage pattern of poly(ADP-ribose) polymerase-1 (PARP-1) were compared among the cells treated with CCl_4, STS and tumor necrosis factor α (TNFα). STS induced caspase-3-like activity at 4 h, with a plateau reached at 6 h, but CCl_4 had no effect even at 8 h (Figure 1b). DNA fragmentation was detected at 6 h and clearly observed at 8 h in STS-treated, but not CCl_4-treated cells (Figure 1c). TNFα with cycloheximide (CHX) is known to induce apoptosis in HepG2.[36,37] PARP-1, a target of caspase-3, was cleaved into apoptotic fragments including the 85 kDa polypeptide in cells treated with TNFα/CHX (Figure 1d, indicated by an asterisk). In contrast, a fragment of 50 kDa, derived from PARP-1, clearly appeared in the CCl_4-treated cells at 4 h and decreased at 8 h (Figure 1d, indicated by an arrow). The 50 kDa fragment was designated as a major necrotic fragment.[38–40] From these results, we confirmed that the death of HepG2 cells induced by CCl_4 is predominantly due to necrosis.

Protection of HepG2 from TNFα/CHX-induced apoptotic death by FNK transduction

PTD-FNK was shown to readily enter cultured cells of a neuroblastoma, SH-SY5Y, in 30 min to 1 h in a previous study.[18] A pleiotropic cytokine, TNFα, has been shown to induce apoptosis and be involved in acute CCl_4-induced hepatic injury.[41–43] We investigated whether PTD-FNK prevents HepG2 from TNFα/CHX-induced apoptosis. Cells were pretreated with PTD-FNK and incubated with TNFα/CHX in the presence of PTD-FNK. PTD-FNK significantly protected HepG2 against the cytotoxicity of TNFα (Figure 2).

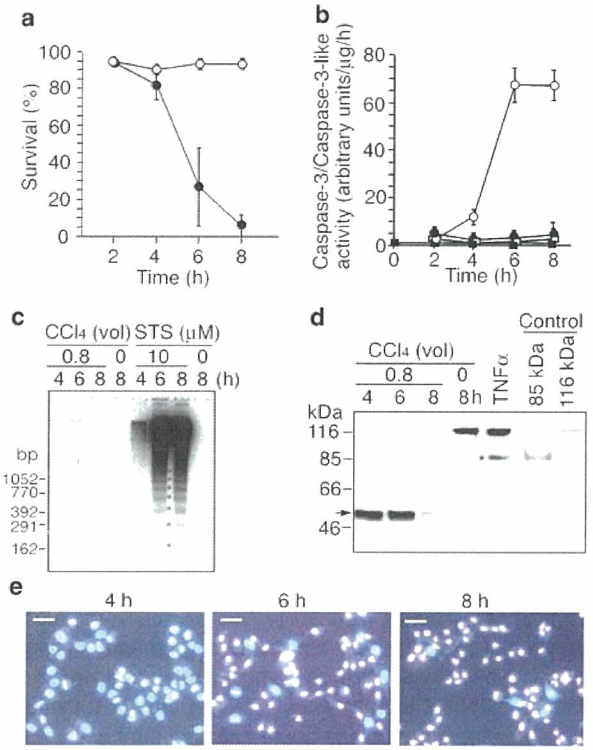

Figure 1 CCl_4 induces necrotic death of HepG2. (**a**) Cells were incubated with DMEM lacking FBS in the presence (closed circle) or absence (open circle) of 80%-saturated CCl_4 for the indicated time periods. The cells were stained with Hoechst 33342 and PI to calculate survival (%); 100 × Hoechst-stained cells/(Hoechst-stained cells + PI-stained cells). The mean of four independent wells (four fields of view per well) is shown with the S.D. (vertical bars). (**b**) Cells were incubated with the complete medium in the presence (open circle) or absence (closed circle) of STS, or with DMEM lacking FBS in the presence (open square) or absence (closed square) of 80%-saturated CCl_4 for the indicated time periods. The cells were harvested to prepare cell lysates for the caspase-3/caspase-3-like activity assay. The enzyme activity (mean with S.D.) is shown as arbitrary units/mg protein/h. (**c**) Cells were treated with CCl_4 or STS as described in (**b**). The harvested cells were treated with Triton X-100, and then centrifuged to remove intact nuclei. After propanol precipitation, fragmented DNAs were subjected to agarose gel electrophoresis. The STS-treated cells (8 h) showed a clear DNA ladder (marked with stars). (**d**) Western blot analysis of PARP. Total proteins were prepared from cells treated with CCl_4 for 4, 6 and 8 h, cells treated with DMEM for 8 h and cells treated with TNFα (10 ng/ml) and CHX (10 μg/ml) for 7 h, as described in Materials and methods. The total protein (30 μg) was subjected to Western blot analysis using an anti-body against PARP. Jurkat control lysate (BD Biosciences Pharmingen) and HL-60 cell extract (induced by etoposide) (Calbiochem), were also used for controls of the 116 kDa intact and the 85 kDa fragment of human PARP, respectively. The 85 kDa fragment appeared in the cells treated with TNFα (marked with*). An arrow indicates a 50 kDa fragment derived from PARP. (**e**) Representative images of cells incubated with DMEM lacking FBS in the presence of 80%-saturated CCl_4 for the indicated time periods. The cells were stained with Hoechst 33342 and PI. Scale bars: 50 μm

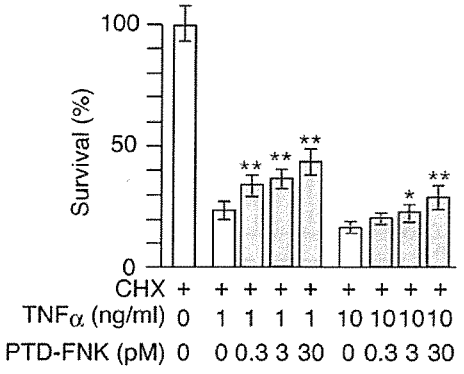

Figure 2 PTD-FNK protects HepG2 against TNFα-induced apoptosis. Cells were washed with FBS-free DMEM, and treated with various concentrations of PTD-FNK in FBS-free DMEM for 1 h, followed by incubation with DMEM containing FBS (10%) and CHX (10 μg/ml) for 30 min. The cells were cultured with TNFα (1 or 10 ng/ml) for 12 h, and cells surviving were enumerated under a microscope by the trypan blue exclusion method. Means of three independent wells are shown with the S.D. Statistical analysis was performed using one-way ANOVA: *, $P<0.05$; **, $P<0.01$, *versus* control

Protection of HepG2 from CCl_4-induced necrotic death by FNK transduction

Next, to examine the cytoprotective effect of PTD-FNK on CCl_4-induced cell death in HepG2, PTD-FNK-pretreated cells were incubated with CCl_4 in the presence of PTD-FNK. Survival rates of the cells treated with PTD-FNK significantly increased up to 3 nM in a concentration-dependent manner and slightly decreased at the higher concentrations (Figure 3a (open bars) and c), indicating that PTD-FNK alone suppresses cell death induced by CCl_4. Comparison of the cytoprotective activity between PTD-FNK and PTD-Bcl-x_L showed that the activity of the former is stronger (Figure 3a and c).

Conversion of necrotic features into apoptotic ones forced by PTD-FNK

During this experiment, we noticed that a substantial population of dying cells treated with PTD-FNK had fragmented nuclei whose morphology was observed when treated with STS (Figure 3c, arrowheads and insets). The population of dead cell carrying a fragmented nucleus increased with the concentration of PTD-FNK, varying from 2.0 to 10% among cells with PTD-FNK treatment (Figure 3a, gray bars).

To confirm whether the dead cells with fragmented nuclei underwent apoptosis, HepG2 cells were exposed to CCl_4 in the presence of Z-VAD-FMK, a cell-permeable pan-caspase inhibitor. Z-VAD-FMK fully inhibited the STS-induced apoptosis of HepG2 (Figure 3c, leftmost panels). Importantly, the survival rate of cells co-treated with PTD-FNK and Z-VAD-FMK was significantly higher than that of cells treated with Z-VAD-FMK alone (Figure 3b). More interestingly, much more of the cells treated with a combination of PTD-FNK or PTD-Bcl-x_L and Z-VAD-FMK were survived than the cells treated with PTD-FNK or PTD-Bcl-x_L alone, and the combination treatment significantly decreased the number of dying cells carrying fragmented nuclei (Figure 3b). These findings strongly suggest that PTD-FNK can protect a majority of HepG2 cells from necrotic death caused by CCl_4, and that PTD-FNK forced the cells in a necrotic pathway into an apoptotic pathway and then Z-VAD-FMK inhibited cell death in the apoptotic pathway.

Furthermore, we tried to detect an early stage of apoptosis by examining the binding of Annexin V to the surface of cells. Cells were exposed to CCl_4 in the absence or presence of PTD-FNK. Some cells were clearly stained with Annexin-V-FLUOS but not with PI (Figure 3e, arrowheads in the lower middle panel). Such Annexin-V-positive and PI-negative cells markedly increased depending upon the addition of PTD-FNK (Figure 3d). In contrast, the Annexin-V-positive and PI-negative population among the cells treated only with CCl_4 was very low and equivalent with that among the cells untreated with CCl_4 (Figure 3d), suggesting that the small population of apoptotic cells was due to the depletion of serum but not by the exposure to CCl_4. Taken together, these results strongly suggest that PTD-FNK leads cells to an apoptotic pathway from the necrotic process induced by CCl_4.

PTD-FNK retains the mitochondrial membrane potential and intracellular ATP level

After entering cells, PTD-FNK localizes to miochondria.[17,18] We examined the levels of intracellular ATP and the mitochondrial membrane potential to reveal the role of PTD-FNK on mitochondrial functions during the protection against necrosis. Exposure against CCl_4 decreased the intracellular ATP and PTD-FNK slightly but significantly suppressed the decrease (Figure 4a). Then, we examined the mitochondria membrane potential in CCl_4-treated cells in the presence or absence of PTD-FNK at 4 h, using mitochondria-specific fluorescent dyes, MitoTracker Red CMXRos and MitoTracker Green FM. MitoTracker Red stains mitochondria, depending upon the membrane potential, while MitoTracker Green FM depends upon the mitochondrial mass in a membrane potential-independent manner. Thus, the relative mitochondrial potential level was estimated by normalizing the red fluorescence with the green one. CCl_4 decreased the membrane potential to 68% of the initial level, and PTD-FNK completely inhibited the decrease (Figure 4b). It is noted that pre-incubation with PTD-FNK did not affect the intracellular ATP levels and the mitochondria membrane potential (Figure 4a and b at 0 time).

Delivery of PTD-FNK into the liver

The tissue delivery of the fused protein, PTD-FNK, injected intraperitoneally (*i.p.*) into 7-week-old male mice was examined by immunohistochemical staining. At 12 h after the injection, exogenous PTD-FNK was detected in the liver by using monoclonal anti-Bcl-x antibody, which recognizes the FNK protein as well as Bcl-x_L (Figure 5a). The protein appeared to be distributed ubiquitously. Next, we tested the delivery of the PTD-FNK protein into liver by injecting subcutaneously (*s.c.*) PTD-FNK. At 1, 3, 5 and 12 h after injection, livers were removed for staining with the monoclonal

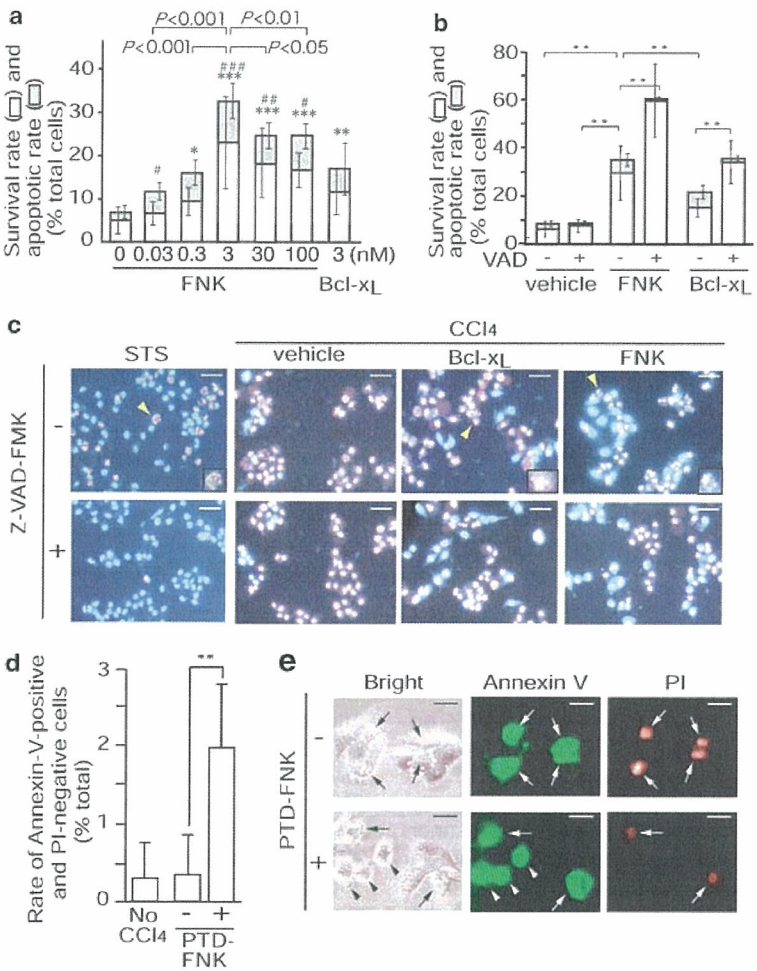

Figure 3 PTD-FNK prevents necrotic death of HepG2. (**a**) Cells were incubated with PTD-FNK (FNK) or PTD-Bcl-x_L (Bcl-x_L) at the indicated concentrations in FBS-free DMEM for 1 h, after washed with FBS-free DMEM. The cells were then treated with 80%-saturated CCl_4 for 8 h in the presence of PTD-FNK (FNK) or PTD-Bcl-x_L (Bcl-x_L) at the indicated concentrations. The cells were stained with Hoechst 33342 and PI to calculate the survival rate (open bar) and apoptotic rate (PI-stained cells with a fragmented nucleus; gray bar) as described in Figure 1a. The mean of four independent wells (four fields of view per well) is shown with the S.D. (vertical bars). Statistical analysis was performed for the suvival rate by one-way ANOVA. *, $P<0.05$; **, $P<0.01$; ***, $P<0.001$, compared with FNK 0 nM.$^{\#}$, $P<0.05$; $^{\#\#}$, $P<0.01$; $^{\#\#\#}$, $P<0.001$, compared with Bcl-xL 3 nM. (**b**) Cells were pre-incubated with vehicle, 3 nM PTD-FNK (FNK) or 3 nM PTD-Bcl-x_L (Bcl-x_L) in FBS-free DMEM in the presence or absence of Z-VAD-FMK (VAD, 50 μM) for 1 h, after washed with FBS-free DMEM. The cells were then treated with 80%-saturated CCl_4 for 8 h in the presence or absence of 3 nM PTD-FNK (FNK), 3 nM PTD-Bcl-x_L (Bcl-x_L) or 50 μM Z-VAD-FMK as indicated. The cells were stained with Hoechst 33342 and PI to calculate the survival rate (open bar) and apoptotic rate (gray bar) as described in Figure 2a. The mean of four independent wells (four fields of view per well) is shown with the S.D.(vertical bars). Statistical analysis was performed for the survival rate using one-way ANOVA: *, $P<0.05$; **, $P<0.001$. (**c**) Representative images of cells described in Figure 2b and cells treated with STS (10 μM) in the presence or absence of Z-VAD-FMK (50 μM) for 12 h. For the cells treated with STS and Z-VAD-FMK, Z-VAD-FMK was added 1 h before the STS treatment. PI-stained cells with a fragmented nucleus are shown by arrowheads and enlarged (insets). Scale bars: 50 μm. (**d**) Cells were pre-incubated with 3 nM PTD-FNK (+) or vehicle (−) in FBS-free DMEM for 1 h, after washed with FBS-free DMEM. The cells pre-treated with PTD-FNK or vehicle were incubated with 80%-saturated CCl_4 containing 3 nM PTD-FNK or vehicle, respectively, for 3 h. Cells without any pre-treatment were also incubated with DMEM lacking FBS (no CCl_4) for 3 h. The cells were stained with Annexin-V-FLUOS and PI to calculate the rate of Annexin-V-positive and PI-negative cells (%); 100 × Annexin-V-positive and PI-negative cells/total cells in a bright field of view. The mean of three independent wells (three to four fields of view per well) is shown with the S.D. (vertical bars). **, $P< 0.0001$ by the Student's *t*-test. (**e**) Representative images of cells described in Figure 2d are shown. Bright, bright field; Annexin V, Annexin-V-FLUOS staining (green); PI, PI staining (red); arrowheads, apoptotic cells; arrows, necrotic or dead cells. Scale bars: 25 μm

anti-Bcl-x antibody. Immunoreactivity was found in the centrilobular region at 1 h and extensive intracellular accumulation of PTD-FNK was observed at 3 h (Figure 5b). The reactivity peaked at 3 h after injection and gradually decreased but clearly remained until 12 h, compared with vehicle injection (Figure 5b and c). Thus, these results indicate that PTD-FNK is promptly delivered to liver by *s.c.* injection as well as *i.p.* administration.

Pre-treatment with PTD-FNK prevents acute liver injury induced by CCl_4

To assess the activity of FNK delivered into the liver to inhibit acute and chronic CCl_4-induced injuries, mice injected with the PTD-FNK protein were treated with CCl_4. Injection of CCl_4 caused a variety of toxic changes such as zonal necrosis, hydropic degeneration of cytoplasm or pyknosis/loss of

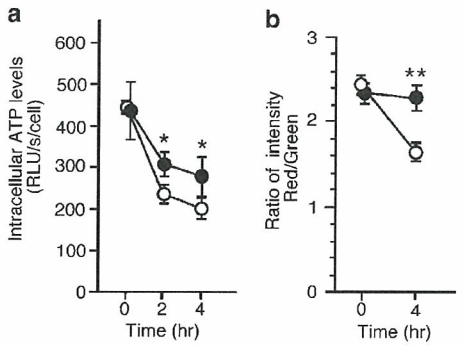

Figure 4 PTD-FNK retains the levels of cellular ATP and the mitochondrial membrane potential in the presence of CCl_4. (**a**) Cells were pre-incubated with 3 nM PTD-FNK (closed circle) or vehicle (open circle) in FBS-free DMEM for 1 h, and continued to culture with 80%-saturated CCl_4 containing 3 nM PTD-FNK or vehicle for the periods indicated. The level of Intracellular ATP per cell was determined using luminescence as described in Materials and methods. Mean values of three independent wells are shown with the S.D.(vertical bars). Statistical analysis was performed using one-way ANOVA: *, $P<0.05$, compared with vehicle. (**b**) Cells were pre-incubated with 3 nM PTD-FNK (closed circle) or vehicle (open circle) in FBS-free DMEM for 1 h and cultured with 80%-saturated CCl_4 in the presence of 3 nM PTD-FNK or vehicle for the periods indicated, followed by being stained with MitoTracker Red and MitoTracker Green FM in fresh DMEM for 30 min. The intensity of fluorescence from each cell was imaged by confocal scanning laser microscopy, and analyzed by using the NIH IMAGE program. Values are expressed as a ratio of the intensity in red divided by that in green of each cell. The mean of the cells examined (PTD-FNK at time 0 and 4 h, 415 and 442 cells, respectively; vehicle at time 0 and 4 h, 425 and 372 cells, respectively) is shown with the S.E. (vertical bars). Statistical analysis was performed using one-way ANOVA: **, $P<0.001$, compared with a vehicle control

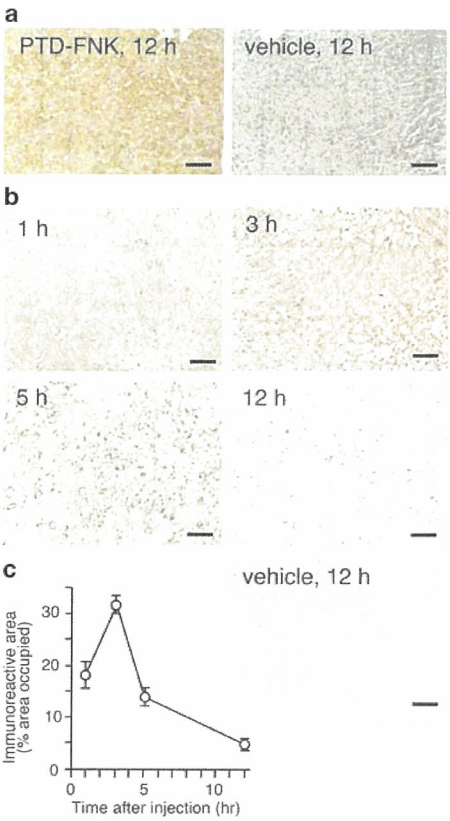

Figure 5 The PTD-FNK protein can be transduced into liver. Male mice (7 weeks old) were injected *i.p.* or *s.c.* with vehicle or PTD-FNK (50 mg/kg). After the indicated periods, the mice were transcardially perfused with cold heparinized physiological saline followed by 4% paraformaldehyde in phosphate-buffered saline (PBS, 0.1 M, pH 7.4), dehydrated and embedded in paraffin. Sections of liver were prepared and subjected to immunohistochemical staining (brown) using anti rat Bcl-x serum. (**a**) *I.p.* injection of PTD-FNK (left) and vehicle (right). Livers were removed at 12 h after *i.p.* These sections were counterstained with hematoxylin (purple) after immunohistochemical staining. Scale bars: 50 μm. (**b**) *S.c.* injection of PTD-FNK. Livers were removed at 1, 3, 5 and 12 h after *s.c.* injection. The immunostained image of liver removed at 12 h after *s.c.* injection of vehicle is also shown. Scale bars: 50 μm. (**c**) Quantitative evaluation of the PTD-FNK remaining in liver after *s.c.* injection. Low-magnification digital images (a half-magnification of (**b**)) of five fields in liver at each time point were analyzed to determine relative areas occupied by Bcl-x immunoreactivity with NIH IMAGE software. The value for liver sections of mice injected with vehicle was used as a background to be subtracted from that for mice injected with the protein. After statistical analysis by one-way ANOVA, the data are shown as means with S.D. (vertical bars). Following the peak at 3 h, PTD-FNK in the liver tissue decreased with a half-span of 3.5 h

nucleus in hepatic cells at both acute and chronic phases (Figures 6c and 7b). A pathologist blindly performed the semi-quantitative histopathological analysis (Table 1).

Pre-injection of PTD-FNK (300 μg/kg) markedly ameliorated this zonal necrosis (Figure 6d and Table 1). Hydropic degeneration of the cytoplasm and pyknosis or loss of nuclei were observed to a small extent in the hepatic cells of mice injected with PTD-FNK, compared to control mice. Serum transaminases, releasing enzymes alanine amino transferase (ALT) and aspartate amino transferase (AST), were measured to evaluate the severity of acute liver injury as a whole (Figure 6a and b). PTD-FNK (300 μg/kg) markedly decreased both activities by two-thirds, compared to vehicle injection. The lower dose of PTD-FNK (75 μg/kg) suppressed the release from liver by one-third compared with the vehicle injection, although the effect was statistically insignificant. The ALT activity decreased at day 2 and was close to a normal level (Figure 7a) on day 3 (data not shown). PTD-Bcl-x_L (300 μg/kg) did not exhibit activity to suppress the release of the enzymes, indicating that PTD-FNK has the stronger activity to protect hepatocytes from cell death induced by CCl_4 *in vivo* as well as *in vitro*.

Post-treatment with PTD-FNK improves acute hepatic injury with a caspase inhibitor

Post-injection of PTD-FNK seemed to only slightly reduce ALT and AST activities in serum (Figure 6a and b), although zonal necrosis was apparently inhibited (Figure 6e and Table 1). The *in vitro* results described above led us to post-inject PTD-FNK with Z-VAD-FMK. The combined post-injection significantly suppressed the elevation of serum ALT and AST, while injection of Z-VAD-FMK alone did not (Figure 6a and b). Histopathological examination also showed that the combined injection profoundly inhibited zonal necrosis (Figure 6f and Table 1). However, no typical apoptotic hepatocyte was found by the TUNEL assay regardless of the injection of PTD-FNK (data not shown).

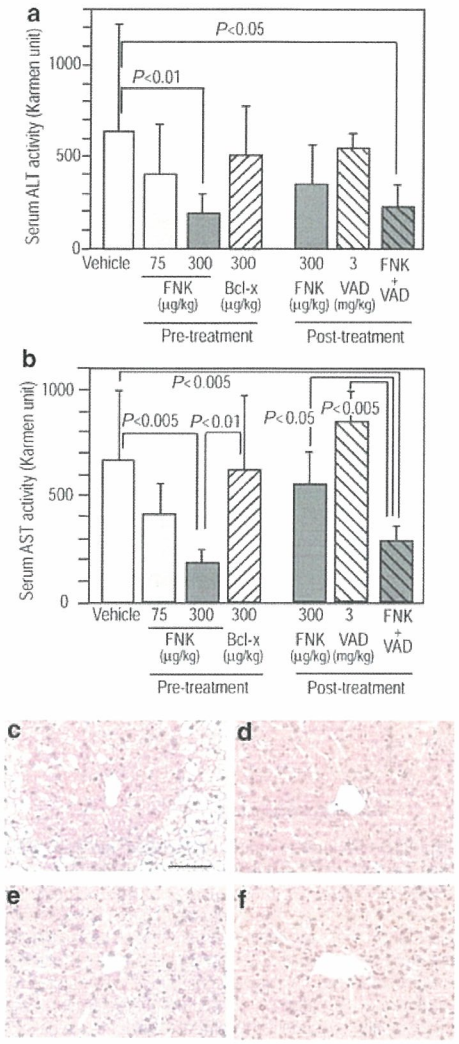

Figure 6 PTD-FNK prevents acute liver injury caused by CCl_4. (**a** and **b**) Animals were *i.p.* injected with vehicle ($n=6$), PTD-FNK (FNK; 75 μg/kg, $n=5$; 300 μg/kg, $n=6$) or PTD-Bcl-x_L (Bcl-x_L; $n=6$) 3 h before the administration of CCl_4 (pre-treatment), or injected with PTD-FNK (FNK; $n=6$), Z-VAD-FMK (VAD; $n=6$) or a combination of PTD-FNK and Z-VAD-FMK (FNK + VAD; $n=6$) 30 min after the administration of CCl_4 (post-treatment). After 20 h, serum (**a**) ALT and (**b**) AST activities were examined and the mean is shown with the S.D. (vertical bars). Statistical analysis was performed using one-way ANOVA. (**c–f**) H&E-stained liver tissue sections in the acute phase. Animals pre-injected with (**c**) vehicle or (**d**) PTD-FNK (300 μg/kg), or post-injected with (**e**) PTD-FNK or (**f**) a combination of PTD-FNK and Z-VAD-FMK, were treated with CCl_4. After 20 h, animals were transcardially perfused with 4% paraformaldehyde to prepare paraffin sections of the liver, which were stained with H&E. Scale bar; 100 μm

Thus, post-injection of PTD-FNK with Z-VAD-FMK greatly exhibited the protective effect for acute CCl_4-induced liver injury to the same extent as pre-injection of PTD-FNK.

PTD-FNK prevents chronic liver injury caused by CCl_4

For chronic liver injury, mice were given CCl_4 twice a week for 1 month. On day 4 after the final administration, livers were

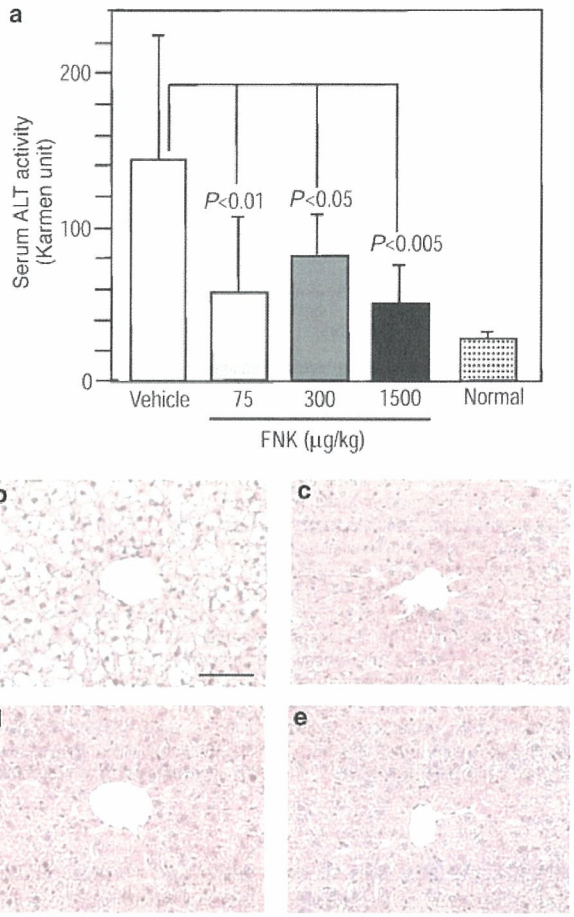

Figure 7 PTD-FNK prevents chronic liver injury caused by CCl_4. (**a**) Animals were *s.c.* injected with vehicle ($n=6$) or PTD-FNK (FNK; 75 μg/kg, $n=5$; 300 μg/kg, $n=6$; 1500 μg/kg, $n=6$) 3 h before the subcutaneous injection of CCl_4, twice a week for a month. On the 4th day after the final administration, serum ALT activity was examined. Normal mice (Normal; $n=6$) without any treatment were also examined. The mean is shown with the S.D. (vertical bars). Statistical analysis was performed using one-way ANOVA. (**b–e**) H&E-stained liver tissue sections in the chronic phase. Animals described in (**a**) were sacrificed on the 4th day after the final administration. Livers were taken out to be fixed with 4% paraformaldehyde and embedded in paraffin. The paraffin sections were stained with H&E. (**b**) vehicle, (**c**) 75 μg/kg, (**d**) 300 μg/kg and (**e**) 1500 μg/kg. Scale bar; 100 μm

histopathologically examined and the ALT activity in serum was measured. Histopathological analysis showed that subcutaneous injection of PTD-FNK (75–1500 μg/kg) exhibited marked protective effects on the toxic changes caused by CCl_4, compared with control mice (Table 1). The serum ALT activity of vehicle-injected mice was five to six times higher than the normal level (normal mice without any treatment) (Figure 7a). In mice injected with PTD-FNK, at 75–1500 μg/kg, the activity of serum ALT was markedly lower than that in vehicle-injected mice. Zonal necrosis in the liver of PTD-FNK-treated mice was clearly reduced (Figure 7b–e and Table 1). Taken together, PTD-FNK mitigated chronic liver injury caused by CCl_4.

Table 1 Histopathological analysis of CCl_4-induced liver injury by a semi-quantitative procedure

			Zonal necrosis				Cytoplasm				Nucleus							
							Hydropic degeneration				Pyknosis				Loss			
	PTD-FNK (μg/kg)	Animal no.	−	+	++	+++	−	+	++	+++	−	+	++	+++	−	+	++	+++
Acute	0	4	0	0	0	4	0	0	0	4	0	0	0	4	0	0	4	0
	300 (pre)	4	4	0	0	0	0	0	4	0	0	0	4	0	2	2	0	0
	300 (post)	6	4	2	0	0	0	0	6	0	0	4	2	0	4	2	0	0
	300 with VAD (post)	6	5	1	0	0	0	5	1	0	0	4	2	0	0	6	0	0
Chronic	0	6	0	0	2	4	0	0	2	4	0	0	0	6	0	0	0	6
	75	5	0	2	3	0	0	0	5	0	0	0	5	0	0	4	1	0
	300	6	0	3	3	0	0	0	6	0	0	0	6	0	0	4	2	0
	1500	6	0	3	3	0	0	0	6	0	0	1	5	0	0	5	1	0

−, no pathological findings; +, mild; ++, moderate; +++, severe

PTD-FNK also prevents liver injury induced by ethanol and dexamethasone (DEX)

Next, we examined whether PTD-FNK is applicable to the other models of hepatic injury. EtOH was injected to generate an experimental model of alcoholic hepatic injury. In fact, it caused many lipid deposits (fatty degeneration) to form in the cytoplasm of hepatic cells and also pyknosis in some cells at 12 h (Figure 8a). Injection of PTD-FNK (20 mg/kg, *i.p.*) inhibited the nuclear degeneration but not the fatty degeneration (Figure 8b and Table 2).

A synthetic soluble glucocorticoid, DEX, is an anti-inflammatory drug but affects some hepatotoxicity.[44] The adverse effect by DEX on the liver was evident (Figure 8c). The DEX treatment markedly resulted in the loss of the eosinophilic compartment from the cytoplasm of hepatic cells, which appeared to represent zonal necrosis, but no cholestasis was observed (Figure 8c). Injection of PTD-FNK (5 mg/kg, *i.p.*) clearly ameliorated the zonal necrosis (Figure 8d) and cytoplasmic and nuclear degeneration (Table 2). As DEX induces apoptosis at high doses, liver sections were stained using the TUNEL assay. In vehicle-injected liver sections, DEX induced many TUNEL-positive cells (Figure 8e), while PTD-FNK reduced the number of TUNEL-positive cells by half, indicating that PTD-FNK prevents DEX-induced hepatic injury. Thus, PTD-FNK seemed to protect hepatocytes against various injuries regardless of apoptosis or necrosis.

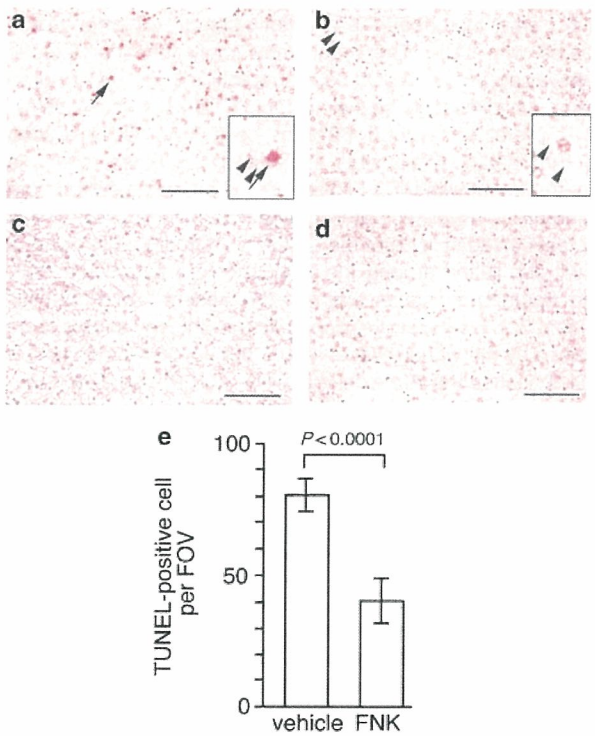

Figure 8 PTD-FNK prevents liver injury induced by ethanol or dexamethasone. Mice were intraperitoneally injected with vehicle or PTD-FNK 3 h before the administration of drugs. (**a** and **b**) Ethanol-induced injury. Mice pre-injected with vehicle (**a**) or PTD-FNK (20 mg/kg) (**b**) were treated with ethanol. After 12 h, animals were transcardially perfused and liver sections were stained with H&E. Arrows and arrowheads indicate pyknosis and lipid deposits, respectively, and have been enlarged in the insets. (**c** and **d**) DEX-induced injury. Mice pre-injected with vehicle (**c**) and PTD-FNK (5 mg/kg) (**d**) were treated with DEX. After 24 h, animals were transcardially perfused and liver sections were stained with H&E. Scale bars: (**a–d**), 100 μm. (**e**) The number of TUNEL-positive cells per high-powered field of view (FOV) in the liver sections prepared from the DEX-treated mice injected with vehicle or PTD-FNK (FNK). TUNEL-positive cells were counted in five non-overlapping fields per slide from each liver ($n=20$ microscopic fields). The vertical bars show the S.D. and statistical analysis was performed using the Student's *t*-test

Discussion

We addressed the question of whether FNK can protect cells from necrotic death via protein transduction technology using the PTD of HIV/Tat.

Under *in vitro* experimental conditions, the addition of 80%-saturated CCl_4/DMEM lacking serum caused death of HepG2 cells with no activation of caspase-3/caspase-3-like activity, no nuclear fragmentation, no ladder formation of DNA in 8 h, and no binding to Annexin V in the early stage. Detection of a 50 kDa fragment derived from PARP-1 in CCl_4-treated cells is strong evidence for necrosis, because the apoptotic PARP-1 fragment of 85 kDa induced with TNFα/CHX is distinct from the 50 kDa fragment[38,39] (Figure 1d). These results clearly

Table 2 Histopathological analysis of ethanol (EtOH)- or dexamethasone (DEX)-induced liver injury by a semi-quantitative procedure

			Zonal necrosis				Cytoplasm								Nucleus							
							Hydropic degeneration				Fatty degeneration				Pyknosis				Loss			
	PTD-FNK (mg/kg)	Animal no.	–	+	++	+++	–	+	++	+++	–	+	++	+++	–	+	++	+++	–	+	++	+++
EtOH	0	4	4	0	0	0	4	0	0	0	0	0	4	0	0	4	0	0	4	0	0	0
	20	4	4	0	0	0	4	0	0	0	0	0	4	0	4	0	0	0	4	0	0	0
DEX	0	4	0	0	0	4	0	0	1	3	4	0	0	0	0	0	1	3	0	0	4	0
	5	4	0	4	0	0	0	0	4	0	4	0	0	0	2	2	0	0	4	0	0	0

–, no pathological findings; +, mild; ++, moderate; +++, severe

indicated that a majority of HepG2 cells exposed to CCl_4 died in a necrotic manner, with a good agreement with previous results.[45] The results of the application of PTD-FNK and PTD-Bcl-x_L have two implications. The first is that PTD-FNK significantly protected the cells from necrotic death induced by CCl_4, compared with PTD-Bcl-x_L. The second is that PTD-FNK clearly increased the apoptotic population among cells treated with CCl_4. The result may imply that the necrotic pathway activated by CCl_4 uses apoptotic mediator(s) in some steps, as discussed below. In fact, PTD-FNK with Z-VAD-FMK protected around 60% of cells from CCl_4-induced necrotic death. A plausible explanation for these results is that treatment with PTD-FNK or -Bcl-x_L caused a switch from a necrotic to apoptotic pathway and that, in turn, Z-VAD-FMK protects these cells from the apoptosis. On the other hand, a small population among the HepG2 cells treated with CCl_4 had fragmented nuclei even in the absence of PTD-FNK (Figure 3a). However, the apoptotic morphology seems to be caused by the withdrawal of serum but not by the addition of CCl_4 because the Annexin-V-positive and PI-negative population was equivalent between cells treated and untreated with CCl_4 (Figure 3d). In double-positive cells with Annexin V and PI, Annexin V may have entered into cells and bound to phosphatidylserine remaining at inner side of the plasma membrane.[46]

Apoptosis has been distinguished from necrosis by morphological and biochemical characteristics including activation of caspases. Recent evidences showed that some biochemical and morphological characteristics of both modes of cell death can be found in the same cell.[1] It is also argued that physiological cell deaths exist that do not appear to be typical apoptosis or dependent on the caspase activation.[47] Appearance of these complex death forms can be explained by interception of active cellular death processes by, for example, oxygen-radical scavengers and inhibition of caspase or PARP.[48–50] Our results support the hypothesis that necrosis and typical apoptosis are two extremes of a spectrum of death programs varying with the strength of the death stimulus.[1] It is noted that mitochondria play an important role in necrosis as well as apoptosis.[1,47] As PTD-FNK was shown to localize in the mitochondria,[17,18] further studies on the function of PTD-FNK would provide insight into the correlation between apoptosis and necrosis. Since FNK exhibited clearer results than Bcl-x_L, FNK will be useful for investigating this issue in future.

How does PTD-FNK protect cells from CCl_4-induced necrosis? The hepatic cell death caused by CCl_4 is clearly due to necrosis (oncosis), although a careful study demonstrated that a small population of hepatocytes undergoes apoptosis in acute CCl_4-induced liver injury.[51] It is generally accepted that CCl_4 is metabolized to the trichloromethyl free radical by the monooxidase system of the ER, where cytochrome P450, mainly isozyme CYP2E1, is thought to play an important role in the pathogenesis.[52] Following production of toxic reactive intermediates, autocatalytic lipid peroxidation is suggested to damage cellular macromolecules, but the cellular mechanisms responsible for CCl_4-induced hepatic cell death are poorly understood.[53] The HepG2 cells used here do not express significant amounts of the enzyme.[54] Since PTD-FNK retained the intracellular level of ATP and mitochondrial membrane potential, the protein seems to preserve functional mitochondria to protect cells.

Another evidence is emerging that calcium ions are involved in the CCl_4-induced cytotoxicity.[53–56] CCl_4 affects intracellular Ca^{2+} content and seems to inhibit differently calcium transport systems on the cytoplasmic, mitochondrial and ER membranes.[56] Calcium ions activate lytic enzymes such as phospholipase A2 that may cause disintegrity of the organelle membrane, including the cytoplasmic membrane.[57] Thus, cytoplasmic Ca^{2+} seems generally to play a key role in necrosis. Interestingly, many studies indicate alterations in the intracellular Ca^{2+} homeostasis to control apoptosis.[58] Bcl-2 inhibits a release of Ca^{2+} from the ER induced by the pro-apoptotic Bcl-2 family members Bax or Bak.[59] PTD-FNK likely inhibits the disruption of Ca^{2+} homeostasis induced by CCl_4 because PTD-FNK affects the cytosolic movement of Ca^{2+} and protects neuronal cells from glutamate excitotoxicity.[18]

PTD-FNK injected into mice was successfully delivered to the liver and prevented the acute and chronic death of hepatocytes caused by CCl_4. On post-injection of PTD-FNK, an injection of Z-VAD-FMK significantly reduced the acute liver injury, as expected from the *in vitro* studies, indicating that the therapeutic window for combined injections extends after the administration of CCl_4. PTD-FNK injection also prevented alchohol- and DEX-induced liver injury. Ethanol was recently shown to generate free radicals in mice and rats,[60,61] increasing the frequency of DNA-strand breaks in the liver.[60] PTD-FNK probably inhibited pyknosis caused by free radicals, while it did not affect fatty accumulation as a

product of the EtOH metabolism. DEX treatment decreases the glutathione concentration in liver[44] and, at a high dose, causes reversible hepatomegaly with hepatopathy.[62] It is also reported that DEX co-administered with methotrexate induced liver damage during a treatment for brain tumor.[63]

This study strongly suggests that PTD-FNK is a potent therapeutic protein to prevent necrotic and apoptotic cell death for emergency care and will allow the development of a novel therapy to prevent cell death by preventing necrosis.

Materials and Methods

Preparation of PTD-FNK

PTD-FNK and PTD-Bcl-x_L were prepared as described previously.[18] In brief, the proteins were recovered as inclusion bodies from *Escherichia coli* cells after treatment with isopropyl 1-thio-β-D-galactoside. The proteins were solubilized in a buffer (7 M urea, 2% SDS, 1 mM DTT, 62.5 mM Tris-HCl (pH 6.8) and 150 mM NaCl), and then subjected to SDS-PAGE to remove contaminating proteins and endotoxin. The gel was treated with 1 M KCl and the transparent band corresponding to PTD-FNK or PTD-Bcl-x_L was cut out. The proteins were electrophoretically extracted from the gel slice in an extraction buffer (25 mM Tris, 0.2 M glycine and 0.1% SDS) for *in vitro* and *in vivo* experiments. The extraction buffer was used as a control (vehicle). The concentration of PTD-FNK or PTD-Bcl-x_L extracted ranged from 1 to 2.5 mg/ml.

Chemicals

CCl_4 and STS were purchased from Wako Pure Chemical Industries Ltd (Osaka, Japan) and Sigma (Sigma-Aldrich Japan, Tokyo, Japan), respectively. Caspase inhibitor I, Z-VAD-FMK, was obtained from Calbiochem (Merck Japan Ltd, Tokyo, Japan). Human recombinant TNFα was purchased from Sigma. Olive oil (Sigma) was used as a solvent of CCl_4 for injection.

Cell culture and drug-inducing cell death

The human hepatoma cell line HepG2 was cultured in DMEM (Life Technologies, Invitrogen, Tokyo, Japan) containing 10% fetal bovine serum (FBS). Cells were plated at 5×10^3 (or 1×10^4) cells/well in a 48-well (or 24-well) IWAKI EZView™ culture plate (Asahi Techno Glass, Tokyo, Japan), which had been coated with collagen type I (Cellmatrix I-P, Nitta Gelatin Inc., Osaka, Japan). After 2 days, the cells were treated with drugs. For CCl_4 treatment, cells were washed with FBS-free DMEM twice and treated with 80%-saturated CCl_4 in DMEM without FBS. FBS-free DMEM was brought to 80% CCl_4 saturation by adding CCl_4-saturated DMEM, where the CCl_4-saturated DMEM was prepared as follows: excess amounts of CCl_4 were added to FBS-free DMEM in a glass bottle and incubated for 15–18 h at 37°C. Hoechst 33342 and PI, 5 μM each, were added to the cells after various incubation periods. To detect cells in the early stage of apoptosis, the cells were stained with Annexin-V-FLUOS (green dye) and PI using a Annexin-V-FLUOS Staining Kit (Roche Diagnostics GmbH, Mannheim, Germany). Annexin-V-positive and PI-negative cells were judged as apoptotic ones. For STS treatment, cells in DMEM with FBS were treated with 10 μM STS. For TNFα treatment, cells in DMEM with FBS were pretreated with CHX (10 μg/ml) for 30 min, and then TNFα was added at the concentration of 1 and 10 ng/ml.

Caspase-3/caspase-3-like activity assay and DNA fragmentation

HepG2 (1×10^5) cells were plated in a 60-mm glass dish coated with collagen type I. After 2 days, the cells were treated with CCl_4 or STS for various periods as mentioned above. Harvested cells were lysed and a caspase fluorescence assay was performed using Ac-DEVD-AMC (*N*-acetyl-Asp-Glu-Val-Asp-7-amino-4-methylcoumarin), with or without the inhibitor Ac-DEVD-CHO (*N*-acetyl-Asp-Glu-Val-Asp-CHO (aldehyde)), and a Caspase Fluorescent (AMC) Substrate/Inhibitor QuantiPack™ (BIOMOL Research Laboratories Inc., PA, USA). Protein concentration was determined with the BCA Protein Assay (Pierce, IL, USA) using BSA as a standard. For the detection of DNA ladders, harvested cells were lysed with 0.5% Triton X-100, and then centrifuged to remove intact nuclei as reported previously.[64] After digestion with proteinase K and RNase A, fragmented DNA was precipitated with 2-propanol. DNA from 0.6×10^5 cells was subjected to electrophoresis on a 2% agarose gel, stained with SYBR Green (Molecular Probes Inc., OR, USA). With this method, DNA from intact nuclei was excluded, and thus the intact DNA did not disturb the pattern of electrophoresis.

Western blot analysis

Cells were harvested and washed. The total protein was solubilized in the presence of 2% SDS by sonication. Protein concentration was determined with the BCA Protein Assay (Pierce) using BSA as a standard. After separated on a SDS-polyacrylamide gradient (4–20%) gel, the proteins were transferred onto a PolyScreen polyvinylidiene fluoride membrane (NEN Life Science Product Inc., Boston, MA, USA). The membrane was treated with anti-human PARP (clone 7D3-6; BD Biosciences Pharmingen, San Diego CA, USA). The intact form and digested products of PARP-1 were visualized with a fluoro bioimaging analyzer FLA-2000 (Fuji Photo Film, Tokyo) using the AttoPhos kit (Roche Diagnostics K.K., Tokyo).

ATP measurement

Cells were plated at 5×10^3 cells/well in a 48-well IWAKI EZView™ culture plate coated with collagen type I. After 2 days, the cells were treated with 80%-saturated CCl_4/DMEM for 0 to 4 h. After the CCl_4/DMEM solution was removed, 100 μl of DMEM without FBS was added to the wells and ATP levels were determined using a 'Cellno' ATP Assay Kit Type N (TOYO B-Net Co., Ltd, Tokyo) as per the manufacturer's instructions. Briefly, 100 μl of the lysis/assay solution provided by the manufacturer was added to the wells. After shaking for 1 min and incubating for 10 min at 23°C, luminescence of an aliquot of the solution was measured in a luminometer, Lumat LB9507 (Berthold Technologies, Berthold Japan Co., Ltd, Tokyo).

Membrane potential measurement

Cells were plated at 1×10^4 cells/well in a 24-well IWAKI EZView™ culture plate coated with collagen type I. After 2 days, the cells were treated with 80%-saturated CCl_4/DMEM for 0 and 4 h. The CCl_4 solution was removed and DMEM containing 100 nM MitoTracker Red CMXRos (Molecular Probes) and 200 nM MitoTracker Green FM (Molecular Probes) was added. After 30-min incubation, fluorescence was imaged by confocal scanning laser microscopy (Fluoview FV/300; Olympus, Tokyo). The Images were analyzed by using the NIH IMAGE program to obtain a ratio of mean intensity in red divided by mean intensity in green of each cell, where the ratio reflects mitochondrial membrane potential of each cell.

Drug-induced liver injury

Male, 4- to 5-week-old C57BL/6N mice (Seac Yoshitomi Ltd, Yoshitomi-cho, Fukuoka, Japan) were used. For acute liver injury induced by CCl_4, mice were *i.p.* injected with CCl_4 (25 mg/kg). After 20 h, blood was obtained for biochemical examinations and mice were perfused transcardially and livers fixed with 4% paraformaldehyde in 0.1 M phosphate buffer (pH 7.4), dehydrated and embedded in paraffin. For acute liver injury induced by ethanol and DEX (Sigma), ethanol (5 g/kg) or DEX (25 mg/kg) was *i.p.* administered. After specified periods, mice were transcardially perfused and livers fixed with 4% paraformaldehyde, dehydrated and embedded in paraffin as described above. For chronic liver injury caused by CCl_4, mice were subcutaneously injected with vehicle or PTD-FNK 3 h before the subcutaneous injection of CCl_4 (25 mg/kg), twice a week for a month. On the 4th day after the final administration, blood was obtained for biochemical examinations and mice were killed. Livers were removed for fixation with 4% paraformaldehyde in 0.1 M phosphate buffer (pH 7.4), dehydrated and embedded in paraffin. Tissues were sectioned (4 μm), and stained with H&E for histopathological analysis. Activities of serum AST and ALT were evaluated using a Transaminase CII Testwako kit (Wako Pure Chemical Industries Ltd). Animal protocols were approved by the Animal Care and Use Committee of Nippon Medical School.

Immunohistochemical staining

The delivery of PTD-FNK into the liver was examined according to the manufacturer's protocol using a Vectastain ABC elite kit (Vector Laboratories, Burlingame, CA, USA) coupled to a diaminobenzidine (DAB) reaction. Rabbit polyclonal anti rat Bcl-x serum (diluted 1 : 250 at 4°C overnight) was used as a primary antibody. In addition, phosphate-buffered saline (PBS) was utilized instead of primary antibody and/or ABC reagent as a negative control.

Terminal deoxynucleotidyl transferase-mediated dUTP nick-end labeling (TUNEL)

Separate sections were used for TUNEL staining using an ApopTag peroxidase *In situ* Apoptosis Detection Kit (Intergen Company, Purchase, New York, USA), and visualized with DAB. For negative controls, terminal deoxynucleotidyl transferase was omitted. In each section, TUNEL-positive cells were counted in five non-overlapping microscopic fields ($\times$ 100 magnification).

References

1. Proskuryakov SY, Konoplyannikov AG and Gabai VL (2003) Necrosis: a specific form of programmed cell death? Exp. Cell Res. 283: 1–16
2. Nathan C (2002) Points of control in inflammation. Nature 420: 846–852
3. Roos KL (1990) Dexamethasone and nonsteroidal anti-inflammatory agents in the treatment of bacterial meningitis. Clin. Ther. 12: 290–296
4. Tracey KJ (2002) The inflammatory reflex. Nature 420: 853–859
5. Palladino MA, Bahjat FR, Theodorakis EA and Moldawer LL (2003) Anti-TNF-alpha therapies: the next generation. Nat. Rev. Drug Discov. 2: 736–746
6. Boise LH, Gonzalez-Garcia M, Postema CE, Ding L, Lindsten T, Turka LA, Mao X, Nunez G and Thompson CB (1993) *bcl-x*, a *bcl-2*-related gene that functions as a dominant regulator of apoptotic cell death. Cell 74: 597–608
7. Minn AJ, Rudin CM, Boise LH and Thompson CB (1995) Expression of Bcl-x_L can confer a multidrug resistance phenotype. Blood 86: 1903–1910
8. Yang J, Liu X, Bhalla K, Kim CN, Ibrado AM, Cai J, Peng TI, Jones DP and Wang X (1997) Prevention of apoptosis by Bcl-2: release of cytochrome *c* from mitochondria blocked. Science 275: 1129–1132
9. Jäättelä M, Benedict M, Tewari M, Shayman JA and Dixit VM (1995) Bcl-x and Bcl-2 inhibit TNF and Fas-induced apoptosis and activation of phospholipase A2 in breast carcinoma cells. Oncogene 10: 2297–2305
10. Fukunaga-Johnson N, Ryan JJ, Wicha M, Nunez G and Clarke MF (1995) Bcl-2 protects murine erythroleukemia cells from p53-dependent and -independent radiation-induced cell death. Carcinogenesis 16: 1761–1767
11. Cory S, Huang DC and Adams JM (2003) The Bcl-2 family: roles in cell survival and oncogenesis. Oncogene 22: 8590–8607
12. Tsujimoto Y, Shimizu S, Eguchi Y, Kamiike W and Matsuda H (1997) Bcl-2 and Bcl-x_L block apoptosis as well as necrosis: possible involvement of common mediators in apoptotic and necrotic signal transduction pathways. Leukemia 11: 380–382
13. Single B, Leist M and Nicotera P (2001) Differential effects of *bcl-2* on cell death triggered under ATP-depleting conditions. Exp. Cell Res. 262: 8–16
14. Asoh S, Ohtsu T and Ohta S (2000) The super anti-apoptotic factor Bcl-xFM constructed by disturbing intramolecular polar interactions in rat Bcl-x_L. J. Biol. Chem. 275: 37240–37245
15. Nagahara H, Vocero-Akbani AM, Snyder EL, Ho A, Latham DG, Lissy NA, Becker-Hapak M, Ezhevsky SA and Dowdy SF (1998) Transduction of full-length TAT fusion proteins into mammalian cells: TAT-$p27^{Kip1}$ induces cell migration. Nat. Med. 4: 1449–1452
16. Schwarze SR, Ho A, Vocero-Akbani A and Dowdy SF (1999) *In vivo* protein transduction: delivery of a biologically active protein into the mouse. Science 285: 1569–1572
17. Ozaki D, Sudo K, Asoh S, Yamagata K, Ito H and Ohta S (2004) Transduction of anti-apoptotic proteins into chondrocytes in cartilage slice culture. Biochem. Biophys. Res. Commun. 313: 522–527
18. Asoh S, Ohsawa I, Mori T, Katsura K, Hiraide T, Katayama Y, Kimura M, Ozaki D, Yamagata K and Ohta S (2002) Protection against ischemic brain injury by protein therapeutics. Proc. Natl. Acad. Sci. USA 99: 17107–17112
19. Graham SH and Chen J (2001) Programmed cell death in cerebral ischemia. J. Cereb. Blood Flow Metab. 21: 99–109
20. Valencia A and Moran J (2004) Reactive oxygen species induce different cell death mechanisms in cultured neurons. Free Radic. Biol. Med. 36: 1112–1125
21. Lin Y, Choksi S, Shen HM, Yang QF, Hur GM, Kim YS, Tran JH, Nedospasov SA and Liu ZG (2004) Tumor necrosis factor-induced nonapoptotic cell death requires receptor-interacting protein-mediated cellular reactive oxygen species accumulation. J. Biol. Chem. 279: 10822–10828
22. Higuchi M, Honda T, Proske RJ and Yeh ET (1998) Regulation of reactive oxygen species-induced apoptosis and necrosis by caspase 3-like proteases. Oncogene 17: 2753–2760
23. Lee WT, Itoh T and Pleasure D (2002) Acute and chronic alterations in calcium homeostasis in 3-nitropropionic acid-treated human NT2-N neurons. Neuroscience 113: 699–708
24. Zhu LP, Yu XD, Ling S, Brown RA and Kuo TH (2000) Mitochondrial Ca^{2+} homeostasis in the regulation of apoptotic and necrotic cell deaths. Cell Calcium 28: 107–117
25. Gwag BJ, Canzoniero LM, Sensi SL, Demaro JA, Koh JY, Goldberg MP, Jacquin M and Choi DW (1999) Calcium ionophores can induce either apoptosis or necrosis in cultured cortical neurons. Neuroscience 90: 1339–1348
26. Pritchard DJ and Butler WH (1989) Apoptosis – the mechanism of cell death in dimethylnitrosamine-induced hepatotoxicity. J. Pathol. 158: 253–260
27. Fukuda K, Kojiro M and Chiu JF (1993) Demonstration of extensive chromatin cleavage in transplanted Morris hepatoma 7777 tissue: apoptosis or necrosis? Am. J. Pathol. 142: 935–946
28. Grasl-Kraupp B, Ruttkay-Nedecky B, Koudelka H, Bukowska K, Bursch W and Schulte-Hermann R (1995) *In situ* detection of fragmented DNA (TUNEL assay) fails to discriminate among apoptosis, necrosis, and autolytic cell death: a cautionary note. Hepatology 21: 1465–1468
29. Columbano A, Endoh T, Denda A, Noguchi O, Nakae D, Hasegawa K, Ledda-Columbano GM, Zedda AI and Konishi Y (1996) Effects of cell proliferation and cell death (apoptosis and necrosis) on the early stages of rat hepatocarcinogenesis. Carcinogenesis 17: 395–400
30. Noguchi T, Fong KL, Lai EK, Alexander SS, King MM, Olson L, Poyer JL and McCay PB (1982) Specificity of a phenobarbital-induced cytochrome P-450 for

metabolism of carbon tetrachloride to the trichloromethyl radical. Biochem. Pharmacol. 31: 615–624
31. Ahr HJ, King LJ, Nastainczyk W and Ullrich V (1982) The mechanism of reductive dehalogenation of halothane by liver cytochrome P450. Biochem. Pharmacol. 31: 383–390
32. Nastainczyk W, Ahr HJ and Ullrich V (1982) The reductive metabolism of halogenated alkanes by liver microsomal cytochrome P450. Biochem. Pharmacol. 31: 391–396
33. Poyer JL, McCay PB, Lai EK, Janzen EG and Davis ER (1980) Confirmation of assignment of the trichloromethyl radical spin adduct detected by spin trapping during ^{13}C-carbon tetrachloride metabolism *in vitro* and *in vivo*. Biochem. Biophys. Res. Commun. 94: 1154–1160
34. Lai EK, McCay PB, Noguchi T and Fong KL (1979) *In vivo* spin-trapping of trichloromethyl radicals formed from CCl_4. Biochem. Pharmacol. 28: 2231–2235
35. Berger ML, Bhatt H, Combes B and Estabrook RW (1986) CCl_4-induced toxicity in isolated hepatocytes: the importance of direct solvent injury. Hepatology 6: 36–45
36. Jones BE, Lo CR, Liu H, Srinivasan A, Streetz K, Valentino KL and Czaja MJ (2000) Hepatocytes sensitized to tumor necrosis factor-alpha cytotoxicity undergo apoptosis through caspase-dependent and caspase-independent pathways. J. Biol. Chem. 275: 705–712
37. Bai J and Cederbaum AI (2000) Overexpression of catalase in the mitochondrial or cytosolic compartment increases sensitivity of HepG2 cells to tumor necrosis factor-alpha-induced apoptosis. J. Biol. Chem. 275: 19241–19249
38. Gobeil S, Boucher CC, Nadeau D and Poirier GG (2001) Characterization of the necrotic cleavage of poly(ADP-ribose) polymerase (PARP-1): implication of lysosomal proteases. Cell Death Differ. 8: 588–594
39. Shah GM, Shah RG and Poirier GG (1996) Different cleavage pattern for poly(ADP-ribose) polymerase during necrosis and apoptosis in HL-60 cells. Biochem. Biophys. Res. Commun. 229: 838–844
40. Aikin R, Rosenberg L, Paraskevas S and Maysinger D (2004) Inhibition of caspase-mediated PARP-1 cleavage results in increased necrosis in isolated islets of Langerhans. J. Mol. Med. 82: 389–397
41. Horn TL, O'Brien TD, Schook LB and Rutherford MS (2000) Acute hepatotoxicant exposure induces TNFR-mediated hepatic injury and cytokine/apoptotic gene expression. Toxicol. Sci. 54: 262–273
42. Morio LA, Chiu H, Sprowles KA, Zhou P, Heck DE, Gordon MK and Laskin DL (2001) Distinct roles of tumor necrosis factor-alpha and nitric oxide in acute liver injury induced by carbon tetrachloride in mice. Toxicol. Appl. Pharmacol. 172: 44–51
43. Simeonova PP, Gallucci RM, Hulderman T, Wilson R, Kommineni C, Rao M and Luster MI (2001) The role of tumor necrosis factor-alpha in liver toxicity, inflammation, and fibrosis induced by carbon tetrachloride. Toxicol. Appl. Pharmacol. 177: 112–120
44. Madhu C, Maziasz T and Klaassen CD (1992) Effect of pregnenolone-16 alpha-carbonitrile and dexamethasone on acetaminophen-induced hepatotoxicity in mice. Toxicol. Appl. Pharmacol. 115: 191–198
45. Jäättelä M and Tschopp J (2003) Caspase-independent cell death in T lymphocytes. Nat. Immunol. 4: 416–423
46. Vermes I, Haanen C, Steffens-Nakken H and Reutelingsperger C (1995) A novel assay for apoptosis. Flow cytometric detection of phosphatidylserine expression on early apoptotic cells using fluorescein labelled Annexin V. J. Immunol. Methods. 184: 39–51
47. Lockshin RA and Zakeri Z (2004) Caspase-independent cell death? Oncogene 23: 2766–2773
48. Vercammen D, Brouckaert G, Denecker G, Van de Craen M, Declercq W, Fiers W and Vandenabeele P (1998) Dual signaling of the Fas receptor: initiation of both apoptotic and necrotic cell death pathways. J. Exp. Med. 188: 919–930
49. Vercammen D, Beyaert R, Denecker G, Goossens V, Van Loo G, Declercq W, Grooten J, Fiers W and Vandenabeele P (1998) Inhibition of caspases increases the sensitivity of L929 cells to necrosis mediated by tumor necrosis factor. J. Exp. Med. 187: 1477–1485
50. Ha HC and Snyder SH (1999) Poly(ADP-ribose) polymerase is a mediator of necrotic cell death by ATP depletion. Proc. Natl. Acad. Sci. USA 96: 13978–13982
51. Shi J, Aisaki K, Ikawa Y and Wake K (1998) Evidence of hepatocyte apoptosis in rat liver after the administration of carbon tetrachloride. Am. J. Pathol. 153: 515–525
52. Raucy JL, Kraner JC and Lasker JM (1993) Bioactivation of halogenated hydrocarbons by cytochrome P4502E1. Crit. Rev. Toxicol. 23: 1–20
53. Recknagel RO, Glende Jr EA, Dolak JA and Waller RL (1989) Mechanisms of carbon tetrachloride toxicity. Pharmacol. Ther. 43: 139–154
54. Cederbaum AI, Wu D, Mari M and Bai J (2001) CYP2E1-dependent toxicity and oxidative stress in HepG2 cells. Free Radic. Biol. Med. 31: 1539–1543
55. Costa AK, Schieble TM, Heffel DF and Trudell JR (1987) Toxicity of calcium ionophore A23187 in monolayers of hypoxic hepatocytes. Toxicol. Appl. Pharmacol. 87: 43–47
56. Hemmings SJ, Pulga VB, Tran ST and Uwiera RR (2002) Differential inhibitory effects of carbon tetrachloride on the hepatic plasma membrane, mitochondrial and endoplasmic reticular calcium transport systems: implications to hepatotoxicity. Cell Biochem. Funct. 20: 47–59
57. Glende Jr EA and Pushpendran CK (1986) Activation of phospholipase A2 by carbon tetrachloride in isolated rat hepatocytes. Biochem. Pharmacol. 35: 3301–3307
58. Breckenridge DG, Germain M, Mathai JP, Nguyen M and Shore GC (2003) Regulation of apoptosis by endoplasmic reticulum pathways. Oncogene 22: 8608–8618
59. Nutt LK, Pataer A, Pahler J, Fang B, Roth JA, McConkey DJ and Swisher SG (2002) Bax and Bak promote apoptosis by modulating endoplasmic reticular and mitochondrial Ca^{2+} stores. J. Biol. Chem. 277: 9219–9225
60. Navasumrit P, Ward TH, Dodd NJ and O'Connor PJ (2000) Ethanol-induced free radicals and hepatic DNA strand breaks are prevented *in vivo* by antioxidants: effects of acute and chronic ethanol exposure. Carcinogenesis 21: 93–99
61. Kono H, Rusyn I, Yin M, Gabele E, Yamashina S, Dikalova A, Kadiiska MB, Connor HD, Mason RP, Segal BH, Bradford BU, Holland SM and Thurman RG (2000) NADPH oxidase-derived free radicals are key oxidants in alcohol-induced liver disease. J. Clin. Invest. 106: 867–872
62. Verrips A, Rotteveel JJ and Lippens R (1998) Dexamethasone-induced hepatomegaly in three children. Pediatr. Neurol. 19: 388–391
63. Wolff JE, Hauch H, Kuhl J, Egeler RM and Jurgens H (1998) Dexamethasone increases hepatotoxicity of MTX in children with brain tumors. Anticancer Res. 18: 2895–2899
64. Asoh S, Mori T, Hayashi J and Ohta S (1996) Expression of the apoptosis-mediator Fas is enhanced by dysfunctional mitochondria. J. Biochem. (Tokyo) 120: 600–607

シンポジウム

ミトコンドリア異常症の治療戦略

太田成男
日本医科大学大学院医学研究科加齢科学専攻
細胞生物学分野

要旨：ミトコンドリア異常症MELASとMERRFの原因としてミトコンドリアtRNA遺伝子変異が同定されたのは15年前である。遺伝子変異から、いかに発症するかを分子レベルで明らかにすることによって治療への戦略をたてることが可能になるはずである。筆者らは変異tRNA分子を分離・精製することによって、変異tRNAではアンチコドンのタウリン修飾が欠損していることを明らかにした。このtRNAのタウリン修飾を回復することがMELAS、MERRFの根本治療への道となるであろう。

Key Words: サイブリド，転写後修飾，タウリン，tRNA，ミトコンドリア脳筋症

はじめに

細胞内小器官であるミトコンドリアは好気的な酸化的リン酸化によってエネルギーを産生し、母系遺伝するミトコンドリアDNA (mtDNA)を持つ[1,2]。ヒトmtDNAの長さは16,568塩基対であり、環状2本鎖DNAである(図1)。ミトコンドリアではミトコンドリア独自の蛋白質合成系により、mtDNA上にコードされている13種類の蛋白質を合成される。この蛋白質合成に使われるtRNAは細胞質ゾル（サイトゾル）とは別のtRNAであり、mtDNAに遺伝子がコードされており、22種類のtRNAからなりたっている。またリボソームRNAもミトコンドリア特有のものであり、構成する2つの12S、16Sリボソーマル RNA遺伝子はmtDNA上にコードされている。一方、リボソーム蛋白質、その他の複製、転写、翻訳反応関連因子類は全て核ゲノムにコードされ、サイトゾルで合成されミトコンドリアに移入される。mtDNAにコードされている蛋白質はいずれも呼吸鎖酵素複合体とATP合成酵素のサブユニットであり、ミトコンドリアが細胞、組織、臓器、そして最終的には個体が活動するために必要なエネルギーの大半を生産するために不可欠な構成成分である。mtDNAは組織、細胞によって異なるが1細胞内に数百から数千コピー存在している。核遺伝子とは異なり多コピーなので変異mtDNAと正常mtDNAが混在する場合があり、混在の状態をヘテロプラズミーと呼ぶ。ヘテロプラズミーにおける正常mtDNAと変異mtDNAの比率は多様であり、ミトコンドリア異常症の多彩な臨床症状の原因のひとつでもある[1,2]。

ミトコンドリア異常症の概観

ミトコンドリア異常症、あるいはミトコンドリア病とはミトコンドリア機能異常が第一義的な原因である疾患の総称である[1]。ミトコンドリアはATPを合成しており、ATP合成系と呼吸鎖を構成する蛋白質はmtDNAと核DNAの双方にコードされていてどちらの遺伝子の変異

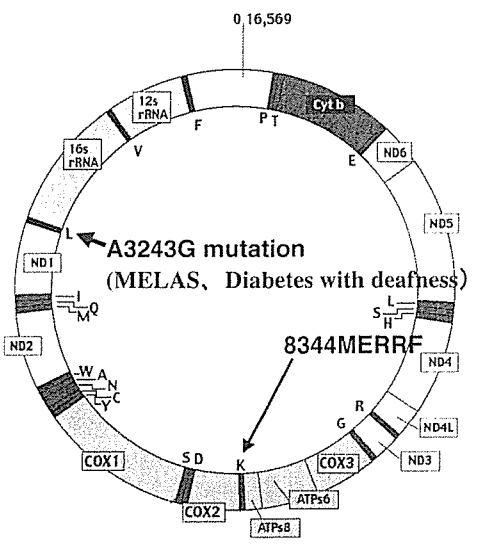

図1　ヒトミトコンドリアDNAの遺伝子配置

ND1、ND2、ND3、ND4、ND4L、ND5、ND6は複合体Iのサブユニット、Cyt bは複合体IIIのサブユニット、CO I、CO II、CO IIIは複合体IVのサブユニット、ATPase6、ATPase8は複合体Vのサブユニットを示す。22種類のtRNA遺伝子はそれぞれ一文字表記アミノ酸で対応する。また12S rRNA、16S rRNAはリボソーマルRNA遺伝子を示す。L（ロイシン）、S（セリン）に対応するtRNAだけは2種類存在する。tRNALeu(UUR)は、UUAとUUGを認識する（R＝A and G, Y＝C and U）。

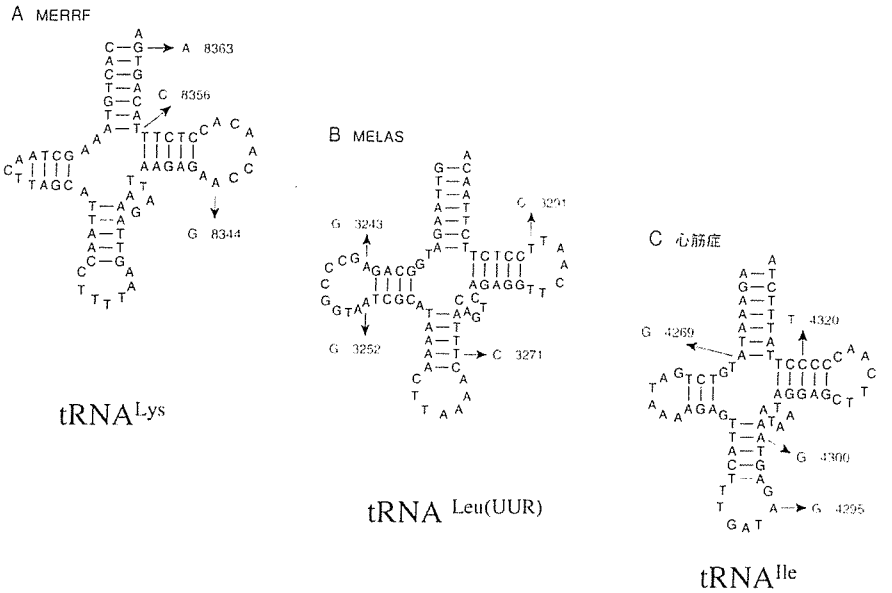

図2　MELAS、MERRF、心筋症患者にみられるミトコンドリアtRNAの変異

A：MERRFはtRNALysの遺伝子の点変異、B：MELASはtRNALeu(UUR)の点変異、C：心筋症はtRNAIleの変異によって発症する。変異の位置に示してある番号はmtDNAの塩基番号。

で起こっていてもミトコンドリアに異常が生じ、いずれの場合もミトコンドリア異常症と呼ぶ。近年では複合的原因の一つであってもミトコンドリア異常が明確である場合にはミトコンドリア病と呼ぶ場合も出てきたように概念が拡張してきている[2]。

mtDNAの変異によって異常が認められるのは、エネルギー需要が大きい骨格筋や中枢神経が中心である。そのため、ミトコンドリア異常によって筋と中枢神経に主に症状が現われる疾患を総称してミトコンドリア脳筋症と呼び、全身に症状があらわれる時はミトコンドリアサイトパチーと呼ぶ。最近はまとめてミトコンドリア病とよぶことが多い。ミトコンドリア脳筋症では、筋力低下、易疲労性、小脳失調がおこる。子供の場合は身長が低い。さらに、痙攣、頭痛、神経性の難聴、痴呆などの症状があらわれることが多い。しかし、必ずしも全ての症状がすべての患者に同様に現われるわけではない。また、酸化的リン酸化の障害を補償するために解糖系が亢進され、最終産物である乳酸が高濃度になるため血液が酸性になる。ミトコンドリア脳筋症の3大病型は臨床症状の特徴の頭文字をとって以下のように名付けられている。外眼筋麻痺を特徴とするCPEO (chroic progressive external ophthalmoplegia)、筋肉の痙攣（ミオクローヌスてんかん）を特徴とするMERRF (myoclonic epilepsy associated with ragged-red fibers)、脳卒中様症状が特徴のMELAS (mitochondrial myopathy, encephalopathy, lactic acidosis and stroke-like episodes)が主な病型である。網膜色素変性と心伝導障害を伴うCPEOはKearn-Sayre症候群として分類され、KSSはCPEOに含まれる。これらの症候群が提唱されたのはそれほど以前のことではなくMELASが症候群としてのはじめて記載されたのは1984年のことである。変異遺伝子が同定されたのは1990年のことであることを考えれば変異遺伝子の同定は極めて速やかだったといえる[3,4]。しかし、変異遺伝子の同定から発症のメカニズムを決定するのにさらに長い時間を要することになった。

CPEOとMERRFの原因遺伝子変異の同定

CPEOはmtDNAの欠失により発症する[5]。その欠失の長さは0.5－8kbpまで様々でその欠失の場所もさまざまであるが、いずれかのtRNA遺伝子部分を欠失しているのが特徴である。瞼が垂れ下がるという眼瞼下垂が病気の特徴であるのもかかわらず、まぶたの筋に欠失mtDNAが多いわけではなく、その特徴を生じさせる原因は今も不明である[6]。mtDNAは母親の遺伝子のみが伝えられる母系遺伝によって子孫へ伝えられることが判明しているが、欠失mtDNAは親には認められないにかかわらず患者の代になって欠失が生じる孤発例がはるかに多い。

MERRFはミオクローヌス癲癇を特徴とし、比較的高齢になって発症する。比較的高齢になってから発症するので遺伝様式は比較的明確にすることができ、母系遺伝である。そのため、mtDNAの変異が原因であることが当初から疑われ、実際、MERRF患者のmtDNA塩基配列を決定することで、ミトコンドリアtRNALys遺伝子の点変異が同定された[7]。興味深いことにMERRF患者からはtRNALysの変異は塩基番号8344だけでなく、8356、8363のいずれにも認められたので、tRNALys遺伝子の変異がMEERFの原因である。ただし、8344変異が患者の大多数を占める。MEERFの変異tRNA遺伝子と変異の場所を図2左に示す。tRNALysの変異によ

って、なぜ、特徴的な痙攣（ミオクローヌス）、が現れるかは不明である。

MELAS、MERRF以外の症状を示すミトコンドリア病で様々なミトコンドリアtRNA遺伝子上の変異が見つかっている[8]。詳しくはMITOMAP、http://infinity.gen.emory.edu/MITOMAP/を参照。また、心筋症では塩基番号4269、4295、4300、4320のtRNAIle遺伝子上に点変異が多く見つかっている（図2右）。

MELASの原因遺伝子の同定

MELASは脳卒中様症状を示す疾患で重篤である。MELASは小児期に発症することが多いので患者の子孫が基本的に存在しないために遺伝様式が明らかではなく、mtDNAの変異によって発症するのかどうか、1980年代当時は予測がつかなかった。mtDNAの塩基配列は個人差が大きく、たとえmtDNAに塩基置換があったとしてもそれが病因であるかどうかをすぐに結論することはできない。病因であるか単なる個人差なのかを明らかにする必要がある。さらに病因である場合でも、正常mtDNAと変異mtDNAが混在していることが多く、変異mtDNAの塩基配列を決定して原因変異を同定しようとしても、たまたま正常mtDNA遺伝子をクローニングしてしまえば変異が見つからない場合もあるかもしれない。

著者らは、自治医科大学小児科桃井真里子教授（現）グループと共同研究で、MELAS患者の筋生検試料から細胞を培養して、細胞をクローン化することに成功した[3,4]。そのために筋細胞の増殖能を増進させるためにSV40 DNAで形質転換させた。そのクローンの中には呼吸鎖活性がある細胞クローンと呼吸鎖活性がない細胞クローンの両者が存在した[4]。すなわち、同一患者の同じ組織から得られた細胞にもかかわらず、呼吸鎖酵素活性が欠損していたクローンと正常なクローンが株化できた。そのふたつの細胞は同一の人に由来するので核は共通であり、mtDNA塩基配列のちがいは個人差に起因しない。このふたつの細胞株から分離したmtDNAに何らかの違いがあればその違いが病因であるはずである。例え変異mtDNAが存在していても、ヘテロプラズミーによって混在している正常mtDNAをクローニングしてしまう可能性もあるので、PCR産物の塩基配列を直接決定した。また、ヘテロプラズミーの程度違いから呼吸鎖活性の違いが生じていないことにも気をつけて、全塩基配列プロファイルを注意深く検討した。以上のような可能性を考えながらそれぞれの株のmtDNAの全塩基配列を決定した。すると、全塩基配列中わずか1カ所のみの塩基配列が異なっていた。そこで、この塩基置換が遺伝子多型でなく病因となる点変異であると結論した。この塩基変異はtRNALeu(UUR)遺伝子上の点変異（塩基番号3243）であった。その後の様々な報告などからMELAS患者の約80％にこの塩基置換が認められた。塩基番号3271、3252や3291のtRNALeu(UUR)遺伝子上の変異をもつ患者もいた。いずれにしてもミトコンドリアtRNALeu(UUR)遺伝子上に変異があるのが特徴である（図2中央）。

サイブリドの作製法の開発

細胞には核ゲノムとミトコンドリアゲノムの二つが共存する。ミトコンドリア遺伝子に変異があり原因であるとしても、必要十分条件ではない。核遺伝子とミトコンドリアゲノムの双方に変異があってはじめて発症する可能性も否定できない。そこで、正常型mtDNAと変異mtDNAによる違いだけを明確にするためには、共通の核をもつ細胞間で比較しなければならない。すなわち、mtDNAの変異が病気の本質的原因であることを証明するため患者細胞の核の影響を排除しなければならない。つまり患者由来の変異mtDNAを持ち、かつ患者由来ではない共通の核を持つ細胞を人為的に作成することが必要である。mtDNAが完全に消失したHeLa細胞（ρ^0細胞）と脱核した患者の細胞（細胞質）を融合することによって、核はHeLa細胞、mtDNAは患者由来の細胞を作成することが可能であると考えた[1,9]。

そこで、筑波大学の林純一教授（現）と共同で、まずmtDNAが完全に消失したHeLa細胞を分離した。mtDNAの複製にはRNAの鋳型が必要であり、その鋳型をつくるのはmtRNAポリメラーゼである。エチジウムブロマイド(EtBr)はmtRNAポリメラーゼの強力な阻害剤である。酵母のmtDNAはEtBrで処理することによって容易にmtDNAの欠失mtDNAがえられることが知られていたので、それをヒントに、HeLa細胞を長期にEtBrで処理した。ほとんどの細胞はmtDNAの消失によって死滅したが、その中からmtDNAが完全に消失した細胞を分離することができた。

一方、患者の線維芽細胞をサイトカラシンで処理して、細胞骨格のアクチンを脱重合し、遠心によって核を除去した。核は重いので遠心によって細胞からちぎれてしまうのである。核を失った細胞質（サイトプラズム）とmtDNA消失細胞を融合することによって、核はHeLaで、それぞれのmtDNAをもつ細胞を作製することができた。細胞間の融合（Hybrid）ではなく、サイトプラズムと細胞の融合であるので、サイブリドと名付けた（図3）。

実際、変異mtDNAを持つサイブリドを作成すると、欠失mtDNAの場合は明快にtRNA量の減少に伴って減少した蛋白合成量の低下して、酵素活性が定量的に減少した。mtDNAの欠失変異によってtRNAが欠乏してミトコンドリア翻訳反応が停止したのがミトコンドリア異常の原因であることが推察された[9]。

一方、点変異が原因である場合もMERRFの8344点変異、MELASの3243、3271点変異はそれぞれの変異を持つサイブリドが呼吸鎖酵素活性の異常を示したこと

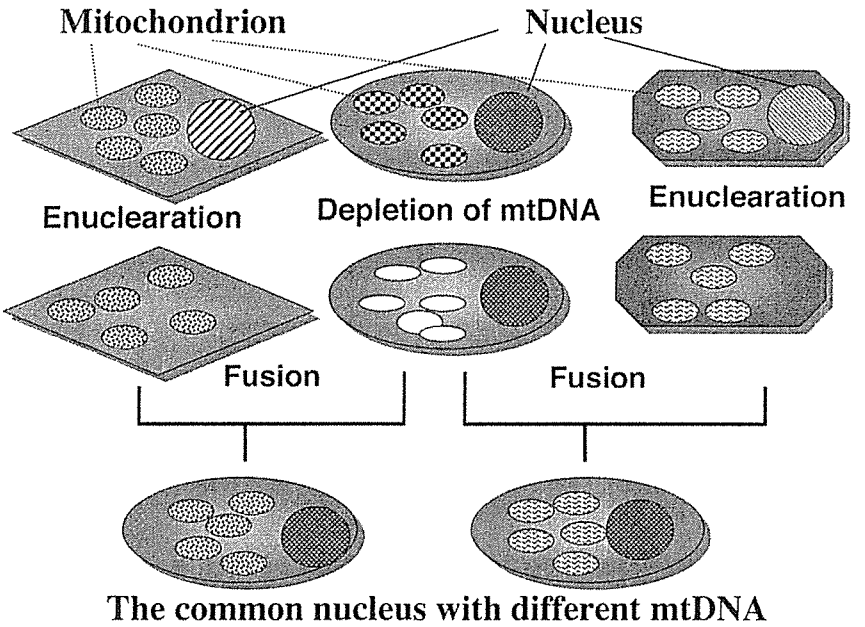

図3　サイブリドの作製法

HeLa細胞からmtDNAを消失した細胞を分離した（中央）。変異mtDNAあるいは正常mtDNAをもつ細胞をサイトカラシンB処理し、遠心することにより脱核する（右と左）。融合することによって、核は共通でmtDNAだけが異なるサイブリドを分離することができる。実際には8-アザグアニン耐性HeLaを用いて、サイブリドを8-アザグアニン存在下で培養してサイブリドを選択する。mtDNAの消失した細胞にもミトコンドリアは存在する。

で病因遺伝子変異であることが証明されたが[10]、具体的にどういうメカニズムで異常が発生したかは欠失の場合のようには簡単に説明がつかなかった。

MERRF患者由来のtRNALys遺伝子（A8344G）変異をもつ場合は、正常のポリペプチドよりも短いポリペプチドが観察されたので、翻訳停止によってprematureな蛋白が生じたものと当初考えられた[11]。しかしながらMELASやMERRFの原因点変異を持つtRNAが具体的にいかにして上記したような異常を引き起こしているかは以前不明であった。

これらの現象を分子レベルで解明するには細胞質のtRNAに比べて存在量が1/100と非常に少ないミトコンドリアtRNAを精製して*in vitro*で解析することが必要であるが、実際に変異tRNAを精製するには技術的に困難で、精製した変異tRNAを用いた解析は長い間行われなかった。

サイブリドは核遺伝子に対するmtDNAの役割を明確にしただけでなく、変異mtDNAの維持を容易にした。例えば患者由来の線維芽細胞が変異mtDNAを持つ場合、SV40遺伝子で形質転換しても細胞分裂寿命がある。しかも我々の用いるHeLa細胞の核をもつサイブリドは細胞寿命がなく無限に増殖させることが可能であるために、大量培養に適している。また、サイブリドを再細胞クローニングすることによって、変異mtDNAと正常mtDNAの比率が様々な細胞株を得ることが可能である。こうして、変異mtDNAに富む細胞株を分離することが容易になり、大量培養も可能になった。また、東大の渡辺研究室では効率よいtRNAの精製法が確立された[12]。大量培養された細胞からミトコンドリアtRNAを精製することが可能になったのである。点変異を持つtRNAの異常なふるまいを明解にするには単一に精製された変異tRNAの解析が必須であり、サイブリドの構築とtRNAの精製法の確立により、精製tRNAを用いたtRNA分子解析の前提条件が揃ったのである。

変異tRNAのアンチコドンの塩基修飾の欠損

一般にRNAの塩基配列はTがUに変わっているだけで鋳型DNAの塩基配列と同じはずある。しかし、tRNAの場合は、転写後にも様々な塩基修飾をうけ変化する。これらのtRNAの修飾塩基には様々な役割がある。tRNAの3次構造を正しく保つ、各種酵素・因子から正確に認識される、コドンの正確な読み分けなどに必要である。特にアンチコドンの修飾塩基はコドンの正確な読み分けに本質的な役割を果たしているので、変異tRNAが正常に修飾を受けているかを解析するのは病因を探るうえで重要であると考えた。アンチコドンはmRNAと結合する3つの塩基であり、mRNAの翻訳に本質的に重要な領域である。多くの修飾塩基の位置、種類はtRNA遺伝子のDNA配列から予測できない。

そこで著者らは東大工学部の渡辺公綱教授（当時）と共同で、変異tRNAを精製することにした。変異tRNAの機能異常を探るため、変異tRNALeu(UUR)(A3243G)とtRNALeu(UUR)(T3271C)[13]、またtRNALys(A8344G)[14]をもつサイブリドを大量培養し、それぞれの変異サイブリ

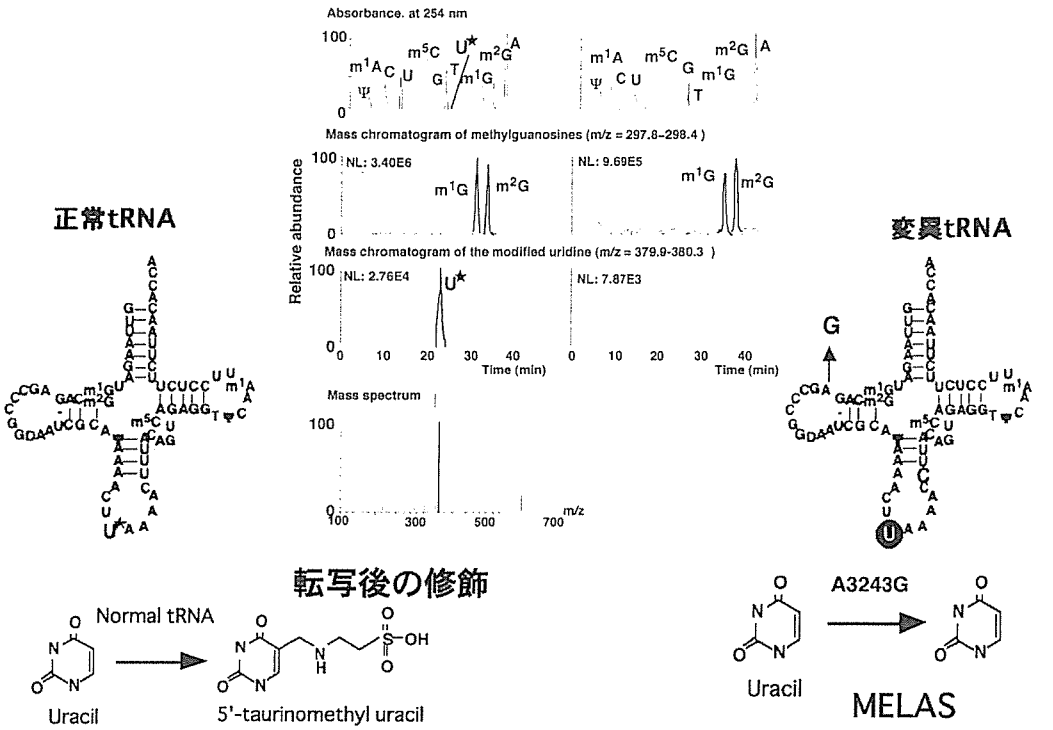

図4　MELAS（A3243G）変異をもつ変異tRNAのアンチコドンのタウリン塩基修飾の欠損

正常ヒトtRNALeu(UUR)とA3243G変異tRNAを精製してアンチコドンの解析を行った。中央はTOF-マススペクトルパターン。正常tRNAにはU*（タウリン修飾U）が検出されるのに対し、変異tRNAではU*が消失している（中央3段目）。一方、m1G（1-メチルG）とm2G（2-メチルG）の修飾は同じ（中央2段目）であるのでタウリン修飾の欠損は特異的である。正常tRNAでは転写後修飾されるのに対し、変異tRNAでは修飾されずUのままとどまる（下図）。（左右のtRNA図：m1G; 1-methylguanosine, m2G; 2-methylguanosine, D; dihydrouridone, ψ; pseudouridine, m5C; 5-methylcytidine, T; ribothymidine m1A 1-methyladenosine U*はタウリンU誘導体）。

ドからtRNAを精製した。まず、カラムクロマトにより分画し、最終的には固相化したオリゴヌクレオチドニハイブリダイズさせて効率よく精製した。そして、その一次構造を決定した。RNA配列解析法であるDonis-Keller法、ポストラベル法や精密質量分析機器LC/MSを用いた核酸分析により、まず野生型のtRNALeu(UUR)とtRNALysの修飾塩基を含む塩基配列を決定した（図4）。すると両方の正常tRNAのアンチコドンの第一文字のU（ウリジン）は修飾されており、当時未知の修飾塩基であった。ところが、3243、3271、8344変異をそれぞれ持つtRNAのアンチコドンの第一文字はいずれも未修飾のUのままで全く修飾されていなかった。他の修飾塩基は変異tRNAと正常tRNAの間で違いは認められず、アンチコドンの塩基のみの特異的欠損であった[13,14]（図4）。同時に、MERRFの8344変異を持つサイブリドではtRNALeu(UUR)は正常に塩基が修飾されていた。また、3243変異をヘテロプラズミー状態で持っているサイブリドでは変異tRNALeu(UUR)と正常tRNALeu(UUR)が混在しており、変異tRNAのみの塩基修飾が欠損していた。これらの知見は変異tRNAにおける修飾欠損が二次的効果ではなく、病因である点変異そのものがアンチコドン修飾酵素の認識を妨げてtRNA分子内のアンチコドンが変化していることを意味していた[13]。その後、この修飾塩基にはタウリンが結合していることがウシtRNAの構造解析から明らかとなった[15]。3243変異と3271変異のMELASの代表的な点変異を持つ二つのtRNALeu(UUR)のどちらにおいてもアンチコドン1文字目はタウリン修飾が欠損していた（図5）。同一tRNA内の異なる位置の点変異により同じ病型を示すのはタウリン修飾の欠損が原因であると示唆された。

患者組織のtRNAの解析

以上のようにHeLa核をもつサイブリド細胞では、tRNA遺伝子の変異によってタウリン修飾が欠損することが明らかとなった。しかし、mtDNAの挙動はしばしば核の影響をうける。そのためHeLaの核の支配によってタウリン修飾欠損が生じるのではないかという可能性も否定できない。そこで、MERRF、MELASの患者組織からtRNAを抽出してタウリン修飾が欠損しているかどうかを調べた（東大　鈴木、新潟県犀潟病院福原らとの共同研究）。患者の組織でも、HeLa以外の核をもつサイブリドでも同じようにMELAS、MERRFの原因点変異によってタウリン修飾が欠損することが明らかになった[16]。以上の結果より、3243変異、3271変異、8344変異によってタウリン修飾が欠損する現象を普遍化することができた。

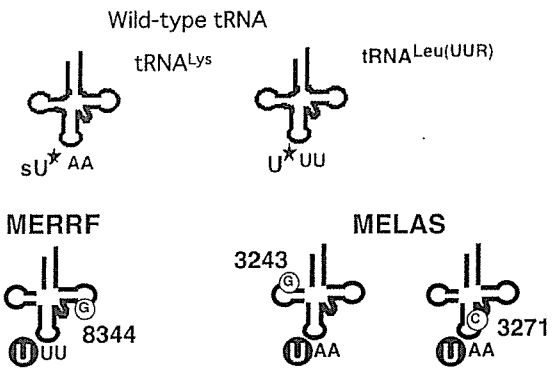

図5　正常tRNALeu(UUR)とtRNALysならびにMELASとMERRFの点変異をもつtRNALeu(UUR)とtRNALysの塩基修飾

正常tRNALeu(UUR)とtRNALysのアンチコドンの第一文字の塩基はタウリン修飾され、さらにtRNALysではイオウが結合している。MELASの3243変異、3271変異、MERRFの8344変異をもつtRNAでは共通にアンチコドンの一文字目が未修飾である。

アンチコドンの修飾欠損と蛋白質合成停止

一種類のtRNA分子が数種類のコドンを認識する機構を一般にwobble（ゆらぎ）塩基対合と呼び、ごく少数の例外を除けば、アンチコドン1文字目に様々な修飾塩基を導入することによって、コドンを効率よく正確に読み分けている[17]。ミトコンドリアtRNAはわずか22種類である。大腸菌のtRNAが85種類もあるのに比べてミトコンドリアtRNAの種類はとても少なく大腸菌のようにひとつのコドンに対して複数のtRNAは存在しない。そのため、ひとつのtRNA種を別のtRNA種で補償することができない。そしてミトコンドリアでは22種類のtRNA種で20種類のコドンを読むためにアンチコドン3文字目に未修飾のUを持つtRNAが8種類存在する。アンチコドンの第1文字目のUは、mRNA側のコドン3文字目がA、G、C、Uいずれでも対合することになる。一方、コドンの第3文字がAかGのものとのみ選択的に対合するtRNAのアンチコドンの第一文字の塩基は修飾されている（tRNALeu(UUR), tRNATrp, tRNALys, tRNAGln, tRNAGluの5種類はU、tRNAMet

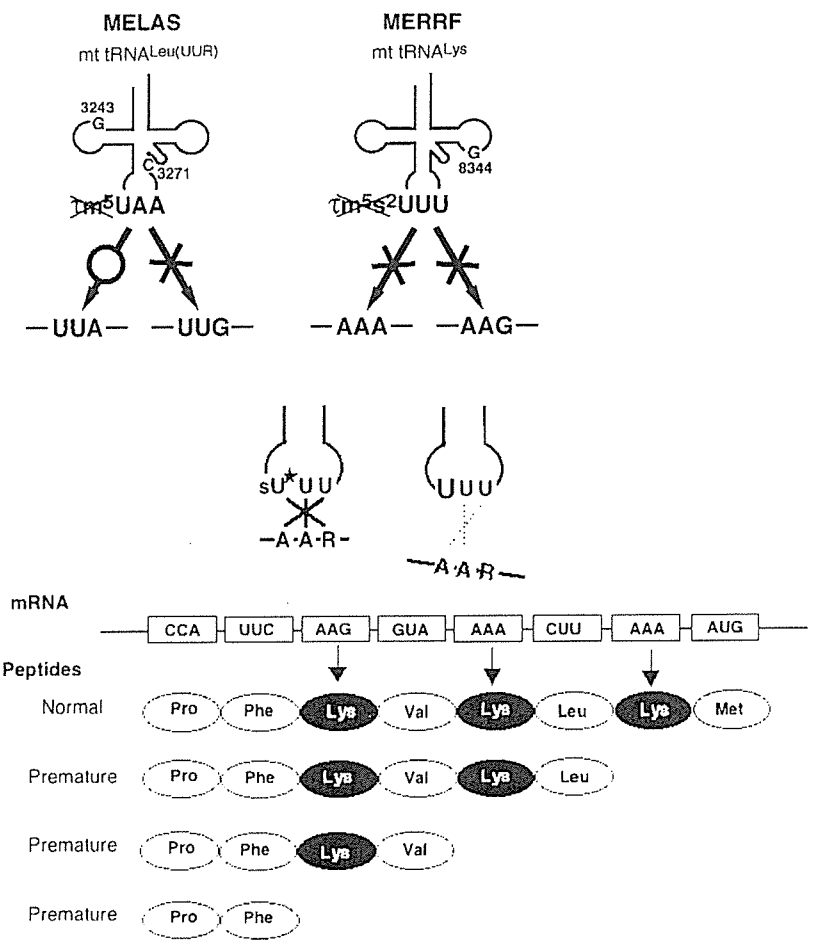

図6　MELAS変異tRNAとMEERF変異tRNAによるコドンの識別

MELAS変異tRNAではmRNAのコドンUUGを読み取ることができず、UUAにのみ結合する。一方、MERRF変異tRNAではAAAとAAGを読みとることができない（上図）。もし、変異tRNALysがコドンAAGかAAAのコドンに遭遇すると蛋白質合成はその場で停止して、途中までできた蛋白質（premature protein）が生成することになる。

はCの誘導体)。これらの塩基認識は、ミトコンドリアwobbleルールとして確立していた[17]。

そのため、前述のミトコンドリアwobbleルールに従って考えてアンチコドンの第1文字のUが修飾されていない変異tRNALeu(UUR)や変異tRNALysは、mRNA側のコドンの3文字目がAGUCのいづれにも結合してしまってまちがったアミノ酸を蛋白質合成の際に導入してしまうことが予測された。tRNALeu(UUR)なら自分のコドンUUA、UUG以外にフェニルアラニンコドンであるUUC、UUUも誤翻訳してしまうことになる。

しかし、さらに研究をすすめると意外にも、変異tRNAは従来のミトコンドリアwobble法則には従わないことが判明した[18,19]。実際にえられた実験結果は、tRNALeu(UUR)やtRNALysのアンチコドン3文字目のUの修飾がコドンとの正確で効率のよい対合を保証するために不可欠であるというものであった。変異tRNALysではAAAとAAGのコドンを読み取ることができず、蛋白質合成が停止する。そのため、合成途中の蛋白質が出現することになる（図6)。この結果はprematureの蛋白質の出現など従来示唆されていた結果と一致するものであった。

分子整形によるタウリン欠損tRNAの機能解析

tRNAのタウリン修飾欠損はtRNA機能の消失につながることが強く示唆されたが、変異tRNAには変異塩基は存在している。そのため、変異塩基が存在せずに、タウリン修飾だけが欠損しているtRNAを用いてtRNA機能を調べる必要があった。そこで、正常tRNAのアンチコドン部分だけをタウリン修飾していない合成RNAと置換した。正常ヒトミトコンドリアtRNAを得るために、ヒト胎盤を用いた。ヒトミトコンドリアtRNAをヒト胎盤より大量に精製して、アンチコドン部を合成RNAに置換することで、タウリン修飾のみを欠損し、その他は正常tRNAと全く同一のtRNAを分子整形法によって人工的に作製した。この結果、変異tRNAの機能不全は変異塩基にあるのではなく、アンチコドンのタウリン修飾の欠損が原因であることが明確になった。さらにtRNALeu(UUR)にタウリン修飾が欠損した場合にはUUAコドンを読み取ることができるが、UUGコドンは読みとることができないことが明らかとなった（図6)[19]。一方、変異tRNALysでタウリン修飾を欠損している場合はAAAとAAGの双方を読みとることができない（図6)[18]。同じタウリン修飾欠損でも、変異tRNAが読み取る範囲が異なるのは興味深い。

タウリンによるミトコンドリア機能回復

変異tRNAのタウリン修飾欠損はMELASとMERRFの根本原因なら培養液にタウリンを加えるとサイブリドのミトコンドリア機能が回復するのではないかという考えが浮かんだ。3243変異、3271変異、8344変異をもつサイブリド細胞（核はHeLa細胞でそれぞれの変異mtDNAをもつように作製した人工細胞）に10mM-60mMのタウリンを加えて1-4日間培養して、ミトコンドリアの機能が回復するかどうかを調べた。ミトコンドリア膜電位はMitotrackerRedの蛍光染色の強度をフローサイトメーターで調べた。酸素消費速度は酸素電極により測定し、ミトコンドリアの形態は共焦点顕微鏡により観察した。ミトコンドリア内タンパク質合成はエメチン存在下でアイソトープメチオニンを取り込ませ、ミトコンドリアを分画後電気泳動によって合成タンパク質を測定した。すると、高濃度タウリン存在下で、MELAS、MERRFの点変異mtDNAをもつサイブリド細胞では、膜電位、酸素消費速度、形態、ミトコンドリア蛋白合成速度、いずれも改善した。40mMのタウリン存在下で4日間培養すると、30%程度酸素消費速度が回復した。タウリン添加によって分子量の大きい蛋白の合成が改善させたので、tRNAの機能が回復したことを示唆する。

しかし、以上の結果は、タウリンが10mM濃度以上の高濃度で効果が見られたので、現実的にタウリンを飲用した時の効果を示すものではない。そこで、細胞内のタウリン合成を抑制するためにタウリン合成の材料であるメチオニンとシステインを必要最小限の濃度として、4日間培養し、その後0.1mM～1 mMの低濃度のタウリンの効果を調べた。すると、特に8344変異を持つサイブリド細胞では、MitoTrackerの蛍光強度が濃度依存的に増加し、形態も糸状になりミトコンドリア機能が回復したことが示唆された（図7)。

タウリン合成を抑制した場合には0.3mM程度の低濃度のタウリンでも十分効果があるので、飲用によってミトコンドリア脳筋症の病態改善に有効である可能性がある。どのような条件下でタウリンが有効であるかをさらに明らかにする必要がある。このタウリンの効果は、変異tRNAにタウリン修飾が回復したためかどうかは現在不明である。別の機構でミトコンドリア機能回復をしている可能性があるが、副作用のないタウリンがミトコンドリア機能回復に一役かってくれれば病態改善の方法として利用できる可能性がある。

tRNA機能回復遺伝子の分離

現在の遺伝子工学の技術では変異mtDNAを正常mtDNAに置換して変異遺伝子を正常化することはできない。mtDNAを導入できるのは現在酵母だけである。また、例え正常mtDNAを導入することができたとしても、ヘテロプラズミー状態になり、変異mtDNAによって最終的に置き換わってしまいかもしれない。理由は不明だが、正常mtDNAよりも変異mtDNAが増加する傾向がある。そこで、現段階ではmtDNAを正常化させて根本治療するという考えは成り立たない。

バクテリアや酵母の遺伝学手法ではrevertant（回復株）あるいはsuppressor mutant（抑圧変異株）を分離